Aalborg University

Model Predictive Control of a Sewer System

Control and Automation:
Master Thesis

Group:
CA10-1030

7 June 2018

Master thesis
Control and Automation
Fredrik Bajers Vej 7
DK-9220 Aalborg Ø, Danmark
http://www.es.aau.dk

AALBORG UNIVERSITY
STUDENT REPORT

Title:

Model predictive control of flow and concentration of sewage in a sewer system

Project period:

P10, Spring semester 2018

Projectgroup:

CA10-1030

Participants:

Jacob Naundrup Pedersen
Thomas Holm Pilgaard

Supervisors:

Carsten Skovmose Kallesøe
Palle Andersen
Tom Søndergaard Pedersen

Abstract:

Copies: TBD
Pages: TBD
Completed: 07-06-2018

Preface

NEW PREFACE !!!!

Units are indicated by sqaure brackets after the parameter has been elaborated e.g. Q is the flow $\left[\frac{m^3}{s}\right]$.

Sources are indicated by [name,year], and can be found in the bibliography list at the given [name,year].

Noget med attachment mappe struktur

Jacob Naundrup Pedersen

Contents

Nomenclature

Abbreviation

Abbreviation	Definition
GIS	Geographically Information System
WATS	Wastewater of Aerobic/Anaerobic Transformations in Sewers
WWTP	Wastewater Treatment Plant
OD	Openings degree
MPC	Model predictive control

Symbols

Symbol	Description	Units
A	Area	m^2
Q	Water flow	m^3/s
q	Inflow of water	m^2/s
q_c	lateral flux input of concentrate	$g/(s \cdot m)$
d	Diameter meter	m
r	Radius	m
F	Force	N
θ	Angle	rad
v	Velocity	m/s
M	Mass	kg
V	Volume	m^3
ρ	Density	kg/m^3
l	Length	m
g	Gravitational acceleration	m/s^2
T	Temperature	$^\circ C$
m	Mass flow	kg/s
ϕ	Flux	g/s
C	Concentrate	g/m^3
R	Hydraulic radius = wetted area / wetted perimeter	m
f	Friction factor	$\cdot$
b	Channel width	m
ω	Angular velocity	rad/s
J	Inertance	kg/m^4
h_n	Head loss	$\cdot$
p	Pressure	Pa
h	Height	m

Introduction 1

Sewers were created to solve the seemingly simple problem of removal of wastewater. The first sewers, registered, dates back to 7000 B.C. in urban settlements and were created to remove wastewater from houses and surface runoff created by precipitation. To avoid clogging and wear of the sewers grit chambers was constructed. They work by slowing the flow of sewage in long narrow channels making the solids, such as sand, end up as sediments in the channels due to gravity. The complexity of sewers increased in ancient Rome where large underground systems were created leading to the main sewer system called "Cloaca Maxima" making it possible to have latrines with running water within households, though mostly made available for the rich [Hvitved-Jacobsen et al., 2013].

During night time the population, without immediate access to a latrine in their household, still disposed waste onto the streets. The reason for this was that they simply did not want to put in the effort to properly dispose of the waste at night. Because of this, the ancient Rome suffered from illnesses related to waste lying in the streets. The hygienic aspect of proper disposal of wastewater in relation to drinking water was not considered until the 19th century, where several European cities saw a large outbreak of cholera causing the deaths of millions [Hvitved-Jacobsen et al., 2013].

The growth in waste furthermore caused the expansion of 26 km sewer network in Paris to 600 km during the 19th century. But it is not until the start of the 20th century that the chemical and microbial processes in sewers are considered. The microbial cause of cholera was identified by the German doctor Robert Koch in 1883, a discovery for which he in 1905 received the Nobel Prize in physiology and medicine. The growing industries and technological progress in the 20th century meant that more chemicals were disposed into the sewers having severe consequences for the organic life downstream of the receiving waters. Wastewater treatment plants were introduced to reduce the pollution, but several countries did not have any wastewater treatment plants before after World War II. Today disposal of sewage and setup of wastewater treatment plants is a given part of a construction of new settlements, even in poor regions of the world [Hvitved-Jacobsen et al., 2013].

1.1 General sewer construction

This section will elaborate on the general construction of sewers. Furthermore, a brief explanation, of the flow into the sewer to the output from the wastewater treatment plant (WWTP), is given.

Generally, sewer construction can be put into two categories which are gravity and pressure sewers. Gravity sewers utilize the topographic advantages of the area in which they are constructed. But in places where the level of the surface area does not accommodate a slope of the sewer pipe, such that wastewater flow in the desired direction, wells with pumps are used to transport the wastewater to an elevated level. An illustration of gravity and pressure sewer lines can be seen in figure 1.1.

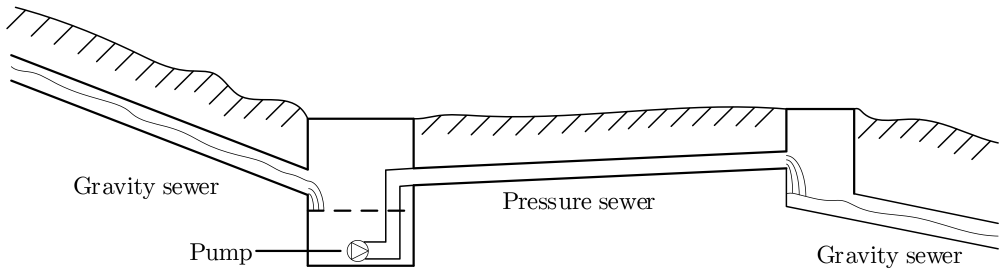

Figure 1.1: Illustration of flow in gravity and pressured sewer lines.

Design of sewer systems involves careful considerations, such that as much of the network utilize gravity for transport of wastewater, to minimize the energy consumption. Therefore, the WWTP is typically located in a low topographic area near a river, fjord or the sea. Other design parameters involve dimensioning of the pipes to avoid overflow and to compensate for groundwater ingress into the sewer lines. Also, the depth should be sufficient, such that subzero temperatures does not prevent the flow in the sewers at any time. Furthermore, the slope of the pipes must be chosen such that sufficient flow is obtained and clogging is avoided. Different materials used to create the pipes gives different amount of friction e.g. a concrete surface will be rougher than polyethylene and thereby have a higher friction. This means that a larger slope of a concrete pipe is needed to avoid clogging. Typically, gravity sewer pipes are made of concrete and pressure sewer pipes of polyethylene [Hvitved-Jacobsen et al., 2013].

In figure 1.2 a block diagram of the flow of wastewater is seen.

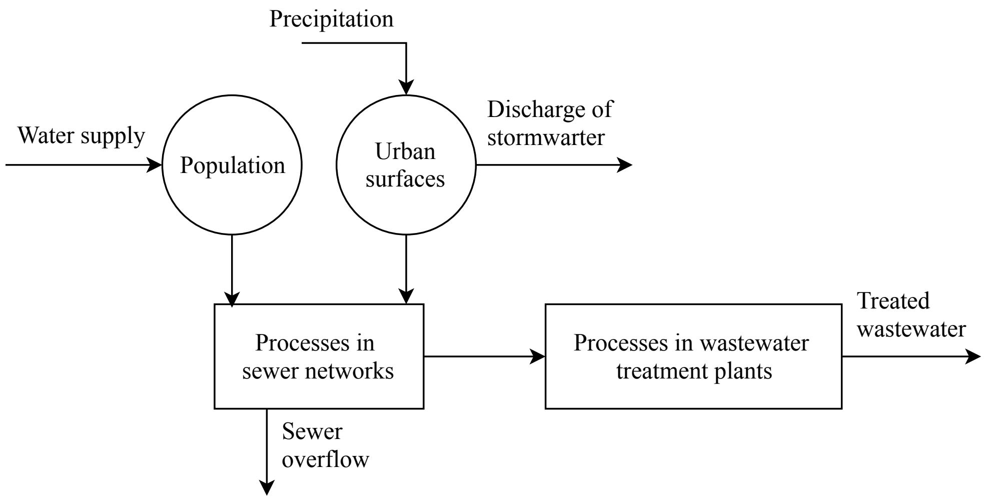

Figure 1.2: General overview of wastewater processes from inputs to treated output [Hvitved-Jacobsen et al., 2013].

Starting at the left side in the figure, precipitation from urban surfaces and roads are let into the sewer by inlets placed at the gutter. In recent times separate sewer systems for surface runoff are constructed, which are also called storm water sewers. The water in these sewers is typically led into stormwater basins, rivers or the sea. In areas with older sewer constructions, storm water is let into sewers where it is mixed with wastewater. The wastewater comes from households or industry disposing of substances of varying consistency. Heavy precipitation can cause the sewers to be filled, and to avoid overflow, into a household or on roads, the wastewater is let into rivers or the sea during such events. The reason for designing storm water sewers is partly to avoid letting untreated sewage into nature, but also to better be able to control the cleansing process at the WWTP. When wastewater is received at the treatment plant it undergoes several processes to separate the unwanted substances from the received wastewater. The cleansed water is then released into nearby rivers or the sea. Due to the sizes of sewer networks, which can have inlets several kilometers from the WWTP, chemical reactions also occur in the sewer pipes [Hvitved-Jacobsen et al., 2013]. The chemical and microbial reactions happening in the sewer lines is discussed in subsection 1.2.1. The processes which the wastewater undergoes at the treatment plant is discussed in subsection 1.2.2.

1.2 Chemical and biological processes

This section will give an overview of the chemical and biological processes that wastewater undergoes from it is led into the sewer till it is cleansed at the WWTP. The various processes occurring at the WWTP is described, to clarify the problems that may arise during operation.

Within wastewater, there is a large number of living organisms. It contains somewhere between 100.000 to 1.000.000 microorganisms per milliliter. These organisms originate from sanitary waste and soil. They are a natural living part of the organic matter and they are an important part of the cleansing at the WWTP. To be able to obtain a high water quality at the output of the WWTP it is necessary to have a thorough understanding of these microorganisms [College, 2018].

Nearly all microorganisms found in wastewater are not harmful and do not cause illness in humans. However, a small group of the microorganisms can cause illness, and these are of great concern in wastewater treatment. The most known diseases to occur are typhoid fever, dysentery, cholera, and hepatitis [College, 2018].

The microorganisms in the WWTP have a specific role in the decomposition of the waste. The three most notable microorganisms in the biological treatment process are bacteria, fungi, and protozoa. The bacteria have the primary role of degrading the wastewater compounds. Bacteria is a single cell organism and is capable of reproducing rapidly when in contact with water. They feed off the waste by absorbing it through the cell wall turning it into sediment solids [College, 2018]. Fungi like bacteria decompose the organic waste, however, they also pose a significant problem for the treatment process as the fungi can proliferate to an extent where it affects the quality of the output from the WWTP [AquaEnviro, 2010]. Lastly, protozoa act as a predator toward the present bacterial population such that it can be controlled [College, 2018]. Reactions in sewer lines is discussed in subsection 1.2.1 and the processes at the treatment plant in subsection 1.2.2.

1.2.1 Chemical reactions in sewer lines

Wastewater is subject to a variety of mass changes in sewers. This is caused by free electrons in the wastewater, which causes chemical reactions and thereby leading to new compounds being created. The chemical reactions occurring is called redox reactions. A Redox reaction is the transfer of electrons between two compounds at an atomic scale. Chemical reactions are determined by the electron acceptors that are present in the wastewater. The electron acceptor is the compound that receives electrons in a redox reaction. Examples of dissolved acceptors are oxygen (O_2), nitrate (NO_3^-) and sulfate (SO_4^{2-}). These acceptors are present, respectively, when aerobic, anoxic or anaerobic conditions exist in the sewer. The redox reaction converts these three compounds in the wastewater to new compounds such as water (H_2O), molecular nitrogen (N_2) and hydrogen sulfide (H_2S) [Hvitved-Jacobsen et al., 2013].

Where redox reactions occur in a sewer line is, to a great extent, determined by the design of the sewer. The aerobic, anaerobic and anoxic conditions do not exist in the same part of the sewer, and the last only occurs if nitrate is artificially added to the wastewater. If the sewer is in an aerobic state then the typical characteristics of the sewer are either partly filled gravity sewer or an aerated pressure sewer. This means that there are free oxygen (O^+) molecules, and these will bind to hydrogen molecules to create water. If the sewer is in an anoxic state, which occurs in pressure sewers, then the addition of nitrate to the wastewater results in molecular nitrogen. If the sewer is in an anaerobic state the characteristic of the sewer is either a pressure line or a full flowing gravity line. Reactions which occurs will result in hydrogen sulfide as the sulfate will bind with the hydrogen molecules. With the knowledge of these condition, sewers can actively be designed to achieve a specific state [Hvitved-Jacobsen et al., 2013]. The two desired states in sewers are aerobic in gravity lines and anoxic in pressure lines to avoid malodorous dissipation into the urban atmosphere.

To model, the chemical and biological reactions in sewer lines a model concept, Wastewater Aerobic/Anaerobic Transformation in Sewers (WATS), is used. The WATS model is expressed as differential mass balance equations which are suitable for numerical computation. It can, therefore, be included in simulations for a specific objective e.g. model of water and gas phase transformations. The WATS model can be applied to a sewer as long as a fundamental understanding of the sewer is available. Whether it is aerobic, anoxic or anaerobic conditions that dominate the sewer, furthermore the soil composition and the pH concentration of the wastewater must also be known and included in the WATS model [Hvitved-Jacobsen et al., 2013].

1.2.2 Wastewater treatment plant

Wastewater from households and industry contains organic and inorganic matter and if it is released into the environment it will result in a polluted environment. This can cause oxygen depletion and thereby affect the wildlife in the water environment negatively. In the following section, the process that wastewater undergoes in a WWTP is elaborated.

In figure 1.3 the various treatments wastewater undergoes is illustrated.

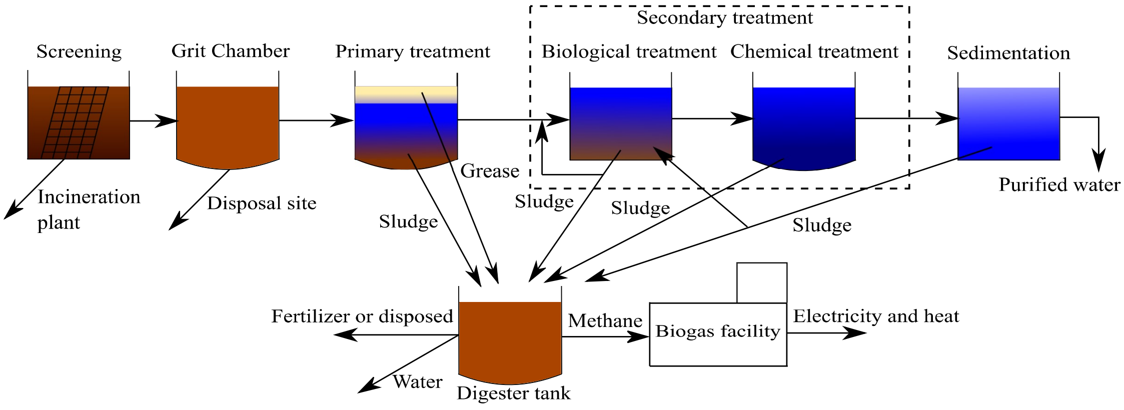

Figure 1.3: General overview of a wastewater treatment plant.

The first stage of cleansing the wastewater is screening, where larger objects are removed from the wastewater which either could cause congestion or damage the equipment. Examples of objects that are filtered from the wastewater are bottles, plastic bags, and diapers [Eschooltoday, 2017]. The wastewater is then lead to the primary treatment, where it first will enter a grit chamber, where objects as sand and stones will settle to the bottom of the tank. These grit chambers are crucial in WWTP that are connected with combined sewer systems. As storm-water may wash sand, stones, and gravel into the sewer these objects will be extracted in this process [EPA, 1994]. The collected objects are disposed at a disposal site. After the screening process the wastewater, still containing organic and inorganic matter, is lead into the primary treatment tank where flow and turbulence are reduced. The organic matter will sediment in the tank, while grease will accumulate at the surface. The grease is scrapped from the surface and lead into the digester tank. The matter that has sedimented is now called sludge or raw primary bio-solids. At the bottom of the tank, large scrappers are moving the sludge to the center of the tank where it is pumped into the digester tank [EPA, 1994].

In the secondary treatment, the wastewater is lead into an aeration tank where the air is pumped in at the bottom. This is called the biological treatment. By aeration of the wastewater, the bacteria gain optimal conditions for respiration. This will speed up the process of decomposing the remaining organic matter from the primary treatment process. In the process of decomposing the organic matter, the bacteria will produce CO_2 that will dissipate into the atmosphere. Furthermore, when the bacteria have consumed the organic matter they will start to produce heavier particles that will sediment in the tank [Rinkesh, 2009]. In figure 1.4 this process is illustrated.

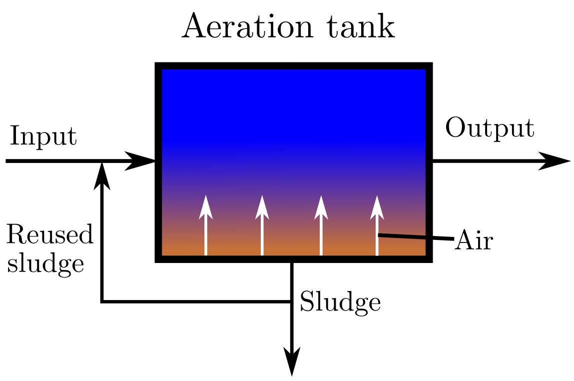

Figure 1.4: Illustration of the aeratation tank in the biological treatment process.

[1] This is called the activated sludge process, because some of the sludge is reused in the aeration phase to retain a high bacteria population. The reused sludge contains millions of microorganisms which increase the efficiency of cleansing the wastewater. After some time the aeration is stopped which causes anaerobic conditions. Other bacteria is then activated in a process called denitrification, where it absorbs oxygen molecules from the nitrate converting it to nitrite. The nitrite flow to the surface in the tank and dissipates into the atmosphere. The remaining sludge that has sedimented is pumped to the digester tank [EPA, 1994,Rossi et al., 2014]. Hereafter a chemical treatment is performed to remove the inorganic matter that is left in the wastewater. Chemicals which is non-damaging to the environment is added to the wastewater. This will create chemical reactions and thereby create new compounds, that will sediment in the tank, which is pumped into the digester tank [Sjøholm, 2016].

After these treatment processes, there are still some particles left in the wastewater. It is therefore lead to a sedimentation tank where the remaining bacteria and sludge will settle before the wastewater is released into receiving waters. The sedimented particles or sludge will either be pumped to the digester tank for further processing or reused in the activated sludge process.

The sludge collected in the digester tank also undergoes further treatment, as the remaining water in the sludge is separated. The water is lead back to the wastewater treatment process where it will undergo the same process again. The sludge then undergoes anaerobic digestion for about a month, where the resulting bio-solids can be used as fertilizer. The methane gas created in the process can be used at a bio-gas facility to produce electricity and heat [Rinkesh, 2009].

1.3 Challenges of wastewater treatment

In the following section various challenges, such as flow and concentrate variations, which affects the treatment efficiency of the WWTP is discussed. Furthermore, this section will mostly be based on information obtained from a meeting with a WWTP, namely Fredericia Spildevand og Energi A/S. A summary of this meeting can be found in appendix A.1. A general daily intake of wastewater from a small town is illustrated in figure 1.5

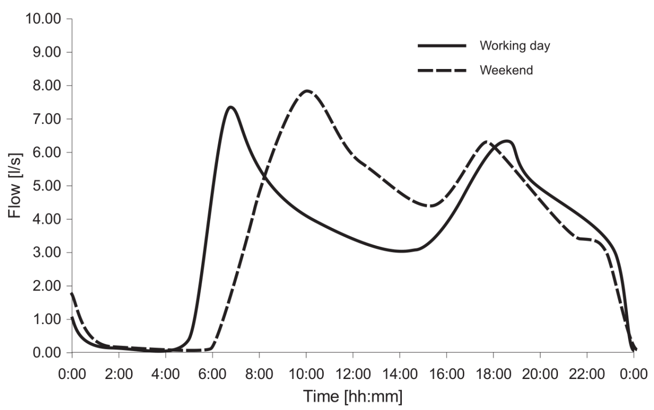

Figure 1.5: Typical daily flow pattern from the town Frejlev, with approximately 2000 residents [Schlütter, 1999].

[1] FiXme Note: Ny tegning

At approximately 06:00 there is a steep increase in flow, which is due to people preparing for work. During the day the flow lessens, until 16:00 where people start returning home from work. The flow increases due to typical household activity such as cooking, bathing, toilets flushing. During night time the flow is at a minimum as most people are at sleep. During weekends the flow patterns change slightly, which could be because of a different sleep pattern than during weekdays.

The flow variations created by human routines is challenging for the treatment process. As mentioned in subsection 1.2.2 sludge is reused to accommodate a sufficient amount of microorganisms to be able to cleanse the wastewater. When a sudden peak in flow occurs, there might not be enough microorganisms available to achieve a satisfying result from the cleansing process. Furthermore, it is not possible to store sludge, with the purpose of using the microorganisms at a later time, as they have a short span of life if the right conditions are not in place.

In Fredericia e.g. there are multiple large companies, which disposes large amounts of wastewater into the sewer. At day to day operation the wastewater flow into the WWTP is not a problem. But random occurrences of sudden large outlets of wastewater from the industry is seen. This could, for example, be from the dairy where a failed batch of cream is let into the sewer such that the tanks can be used to produce a new product. In some cases, the companies contact the WWTP to warn on the incoming amount of wastewater or to agree on the discharge flow of the discarded product. This is not something that the companies are required to do, and does not always happen. This means that the WWTP soonest discovers the added load at the inlet, and therefore has limited possibilities to react on the sudden change of flow. These outlets pose a problem for the WWTP. Not only because of the change in flow, but also because the concentrate of the various compounds in the wastewater is usually higher from the larger companies. Typically, the industry is efficient in letting out wastewater within certain pH levels at reasonable flow levels. The only countermeasure, for these incidents of sudden discharge, is to prevent overflow. This is done by letting some of the wastewater, in the later unfinished stages of the cleansing process, through into the fjord. Furthermore, changes in chloride concentration, from either industry outlets or back-flow from the fjord due to heavy precipitation, is problematic for the bacteria. Meaning that changes in concentrate cause a drop in efficiency until the bacteria have acclimated. Contrary, a static level of chloride does not pose a problem for the bacteria.

To sum up, the typical problems which a WWTP encounters. Flow variations are problematic as the cleansing process reuse sludge. The random changes are either caused by larger industry or as a result of heavy precipitation. Outlets by the industry are more of a concern when considering the concentration of the wastewater. Changes in concentration can cause inefficiency at the WWTP as the bacteria need time to acclimate to changes. Precipitation is a problem as a result of the large increase in flow it causes, which can lead to capacity problems at the WWTP.

1.4 Problem statement

Based on the information in the previous sections, which states that several problems occur during wastewater treatment, the problems can be summed to the following points:

1. Flow variations due to large industries and natural phenomenons
2. Concentration variations due to large industries and natural phenomenons
    a) Chloride variations
    b) Phosphor variations
    c) Nitrogen variations
    d) Organic matter variations

To be able to implement countermeasures towards these problems information is needed about the flow of wastewater in the sewer lines. As measurements is rarely available for entire sewer networks or even parts of it, an ideal solution would be to construct a simulation environment where different scenarios can easily be setup [Fredericia-Spildevand, 2018b]. Furthermore, a control scheme is needed to be able to implement an efficient countermeasure. It has been decided to utilize model predictive control (MPC) as the control scheme for this project. This control scheme excels in obtaining optimal control action when operating systems close to limitations, as constraints can be applied, making it ideal for this project. From this a problem statement can be formulated:

How can a simulation environment be constructed, which mimic the behavior of a real sewer system, where MPC is utilized as the control scheme to obtain stable sewage output such that optimal performance can be obtained from a WWTP.

System description 2

This section will go into details of the structure of the sewer network for which the further work of this project will be based upon.

As mentioned in section 1.3 a steady flow of sewage with a fixed level of contaminants is desired such that an optimal utilization of the wastewater treatment plant can be obtained. An area of interest is Fredericia with a sizable population of approximately 40.000 people and industries where some of the largest consists of a brewery, bottling plant, refinery and a dairy plant [Statistics-Denmark, 2018]. All of these industries are placed at the outskirts of the city, meaning that the wastewater discharged into the sewer goes through populated areas creating an uneven flow of wastewater to the WWTP. Two main sewer lines separates the northern and southern part of the city. To limit the scope of the project only the northern main sewer line is considered. This line covers the largest part of the households and the industry, located in the city. In figure 2.1, a simplified overview is given of the northern main sewer line in Fredericia. The placement of the sewers shown in the figure is obtained from a Geographically Information System (GIS) map, which is made publicly available by the municipal of Fredericia [Fredericia-Spildevand, 2018a]. The red and green lines indicate sewers with flows of wastewater only and combined sewers with flows of wastewater and surface runoff, respectively. The populated areas are indicated by blue and green transparent colors, to easier be able to distinguish between the different parts of the sewer network. The red transparent areas indicate small to medium sized industry. Only the sewer lines out of or between the separate areas are shown. Furthermore, the areas connected by a red line has a separate sewer system for surface runoff, which is lead into various ponds or the sea, minimizing the load on the wastewater treatment plant. The bottling plant, refinery and the brewery is marked by the purple, brown and black rings, respectively. Furthermore, several inlets for surface runoff connected directly to the main sewer line exists.

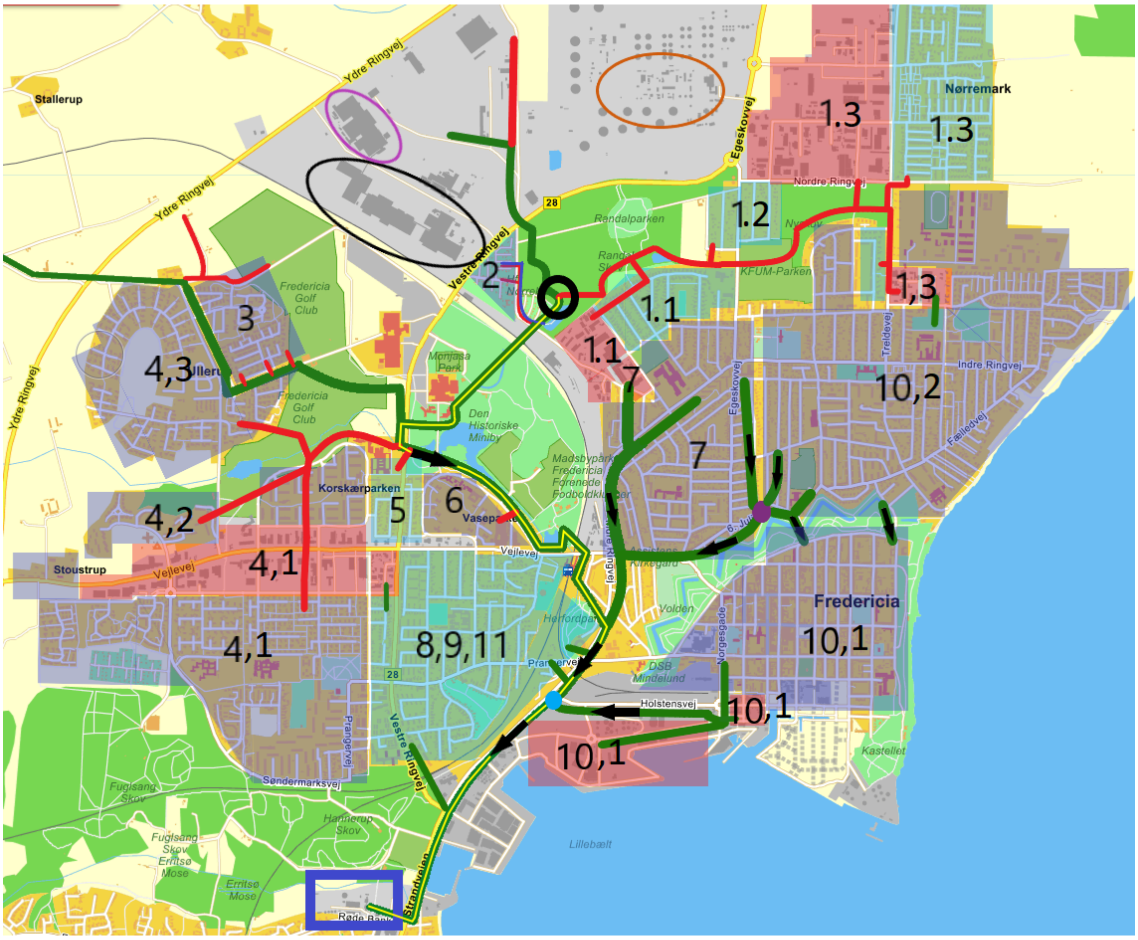

Figure 2.1: Simplified mapping of the northern part of the sewer network in Fredericia. The blue and green transparent colors indicate populated areas and the red transparent area indicate industry. Red and green lines is sewers with flows of wastewater and combined wastewater and surface runoff respectively. Bottling plant, refinery and brewery is marked by purple, brown and black circles respectively. The black circle denotes the starting point of the main sewer line. The green line with a yellow stripe within represent the main sewer line. The purple dot is a connecting point with two incoming and two outgoing sewer lines. The blue dot is a wastewater pumping station which elevates sewage such that gravity can be utilized for the remaining transport into the treatment plant. Blue rectangle marks the location of the wastewater treatment plant [1]. [Eniro, 2018] [Fredericia-Spildevand, 2018a]

The various enumerated parts in figure 2.1 is shown by order of attachment to the main sewer line, together with distance between each attachment, in figure 2.2.

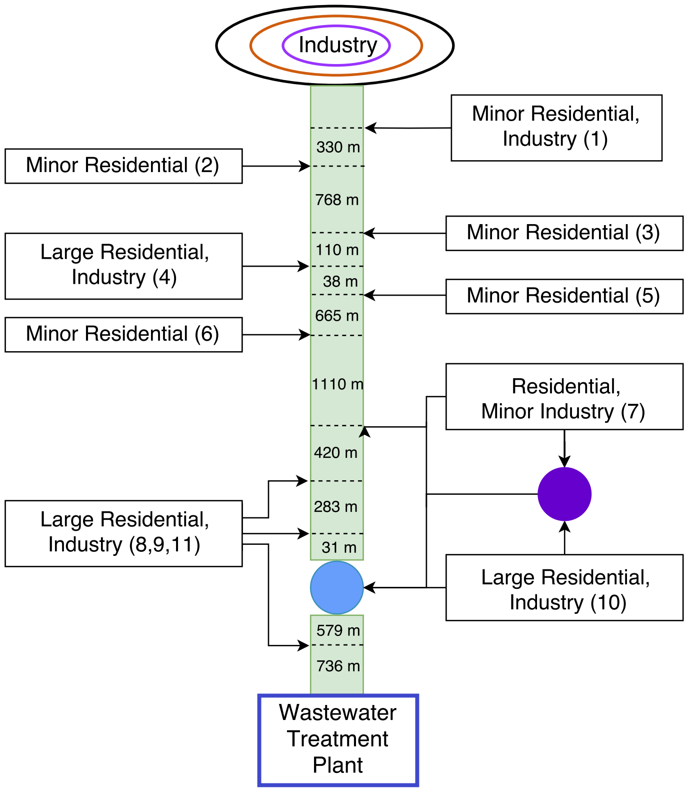

Figure 2.2: Simplification of the attachments to the main sewer line shown in figure 2.1. The numbers correspond to which area is connected to the main sewer line farthest from the wastewater treatment plant, with the distance between them [Fredericia-Spildevand, 2018a].

Furthermore the different sections consist of pipes with varying diameters which can be seen in table 2.1.

Pipe section	Pipe length (meter)	Inner pipe diameter (mm)	Bed datum in (m)	Bed datum out (m)	Bed slope (‰)
1 → 2	303	900	11,56	10,65	3,00
	27	1000	10,65	10,57	3,00
2 → 3	155	1000	10,57	9,94	4,10
	295	800	9,94	6,33	12,20
	318	900	6,33	4,71	5,30
3 → 4	110	900	4,71	4,31	3,60
4 → 5	38	1000	4,31	4,40	-2,40
5 → 6	665	1000	4,40	2,43	3,00
6 → 7	155	1000	2,43	2,31	0,80
	955	1200	2,31	-0,48	2,90
7 → 8	293	1200	-0,48	unknown	
	11	1300	unknown	-1,38	
	116	1200	-1,38	-1,62	2,10
8 → 9	283	1400	-1,62	-2,09	1,70
9 → 10	31	1400	-2,09	-2,15	1,90
10 → 11	125	1600	0,31	0,05	2,10
	94	1500	0,05	-0,07	1,30
	360	1600	-0,07	-1,72	4,60
11 → WWTP	736	1600	-1,72	-2,60	1,20
Total length 1 → WWTP	5070				

Table 2.1: Table of the various lengths and the approximate inner diameter of pipe, appearing in order, in the main sewer line. Pipe section indicate the length of pipe between the attachment of the various areas to the main sewer line [Fredericia-Spildevand, 2018a].

Some assumptions are made to avoid possible complications during simulation. The negative slope of the section between connection point four and five is flipped such that no permanent storage of sewage happens. The reason for this assumption is that it will ease the computation, of the free flow in that section, if storage in the pipe sections could be disregarded during simulation. Furthermore, the new slope is deemed acceptable based on the obtained slopes of the remaining pipe sections. The two pipe sections between point seven and eight, where out- and input datum is unknown, are gathered into a single pipe section. This section will be designated an inner diameter of 1200 mm as the section with the larger diameter, because of its short length, is assumed insignificant when considering the free flow at the end point of the combined section.

Pipe section	Pipe length (meter)	Inner pipe diameter (mm)	Bed slope (‰)
4 → 5	38	1000	2,40
7 → 8	304	1200	3.00
	116	1200	2,10

Table 2.2: New slope values for sections with negative slope and unknown values.

To be able to simulate how the wastewater propagates throughout the main line the flows in each residential and industrial area is needed. However, Fredericia Spildevand og Energi A/S does not have measurements of the flow or concentration from the specific areas. Only at a limited amount of pumping stations, at various positions in the city, are there flow measurements available. Therefore flow profiles for the various inputs shown in figure 2.2 needs to be designed. For this purpose the flow profile seen in figure 1.5 is utilized, for the residential and minor industry areas, as an estimate of the flow during 24 hours. The flow profiles is scaled to fit the size of each area and delayed approximately with the distances to the main line seen in figure 2.1.

From figure 2.2 it can be seen that 11 different flow profiles needs to be constructed to cover each residential and industrial area wastewater contribution to the main line. By knowing the area and density of the population a flow profile can be scaled to each of the residential and industrial areas. On average there is 2,6 residents per house in Denmark which will henceforth be the foundation for obtaining population for the various areas [Nykredit, 2018]. Furthermore, it is assumed that the urban areas one to six together with eight, nine and eleven are single-family houses and zone seven and ten are apartments in buildings with several floors, meaning that area seven and ten has a higher density of population per square kilometers. As the northern part of Fredericia consists of the largest part of the city, the assumption is that around 30.000 of the approximately 40.000 people resides there. The residential area 1,1 is used to obtain an approximately density of people per square kilometer within the urban areas. The number of houses located in this area is found to be 199 which gives an average urban population density of 3098,2 per square kilometer. The approximated size of the various areas is found, and from that the population by multiplying with the average population density. The remaining of the population is divided between area seven and ten. As area seven is approximately a third of the combined area it is given a third of the remaining population leaving the remaining to area ten. In table 2.3 the approximated size of the residential and industrial areas, together with the population of the residential areas, are shown.

Zone	**Residential area** $[km^2]$	**Industrial area** $[km^2]$	**Population per area**
1,1	0,167	0,0083	517
1,2	0,111	-	344
1,3	0,458	0,543	1418
2	0,056	-	173
3	0,167	-	517
4,1	1,125	0,375	3485
4,2	0,167	-	517
4,3	0,580	-	1797
5	0,104	-	322
6	0,115	-	356
7	0,771	0,014	5874
8 - 9	0,667	0,021	2067
10,1	0,903	0,333	3916
10,2	1,781	-	7832
11	0,278	-	865
Total area	7,45	1,294	30000

Table 2.3: Table of the sizes of the residential and industrial areas and the population in the residential areas [Nykredit, 2018].

In figure 2.3 a flow profile is shown for the residential area 1,1.

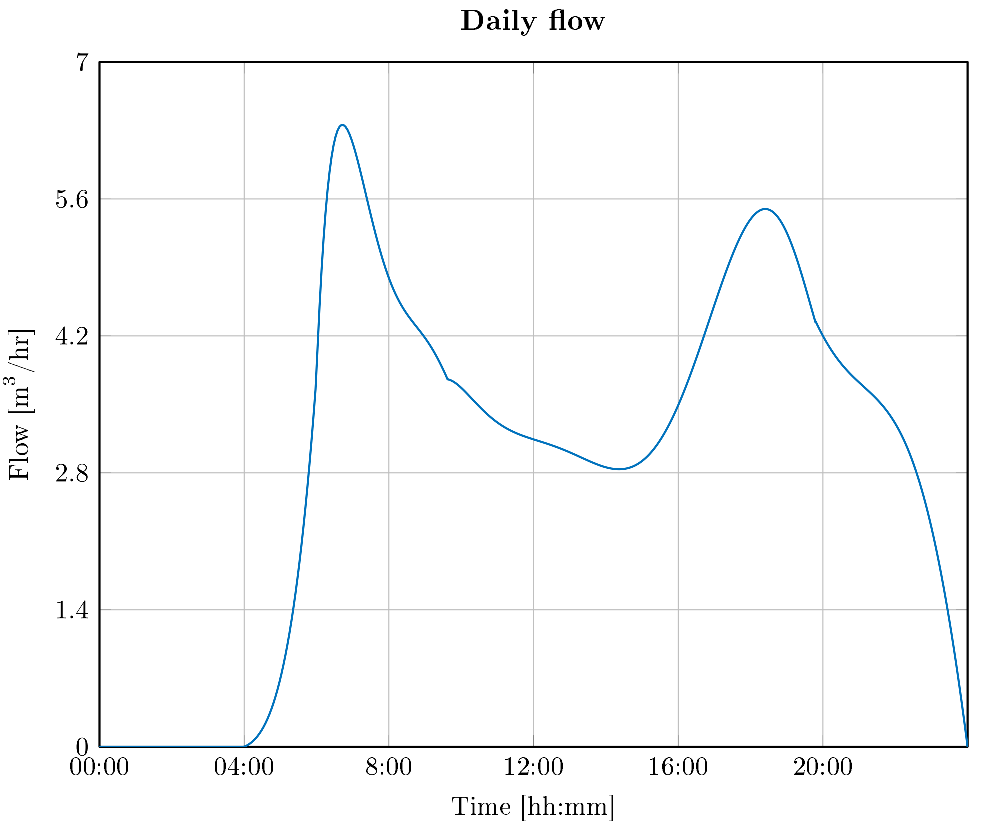

Figure 2.3: Flow profile for the residential area 1,1.

Flow profiles for the various residential and minor industry inputs to the main line and details on the creation of them can be found in appendix A.3.

Lastly profiles are needed from the industry which counts the brewery, bottling plant and the refinery. In figure 2.4 combined flow from the brewery and bottling plant during 24 hours is seen.

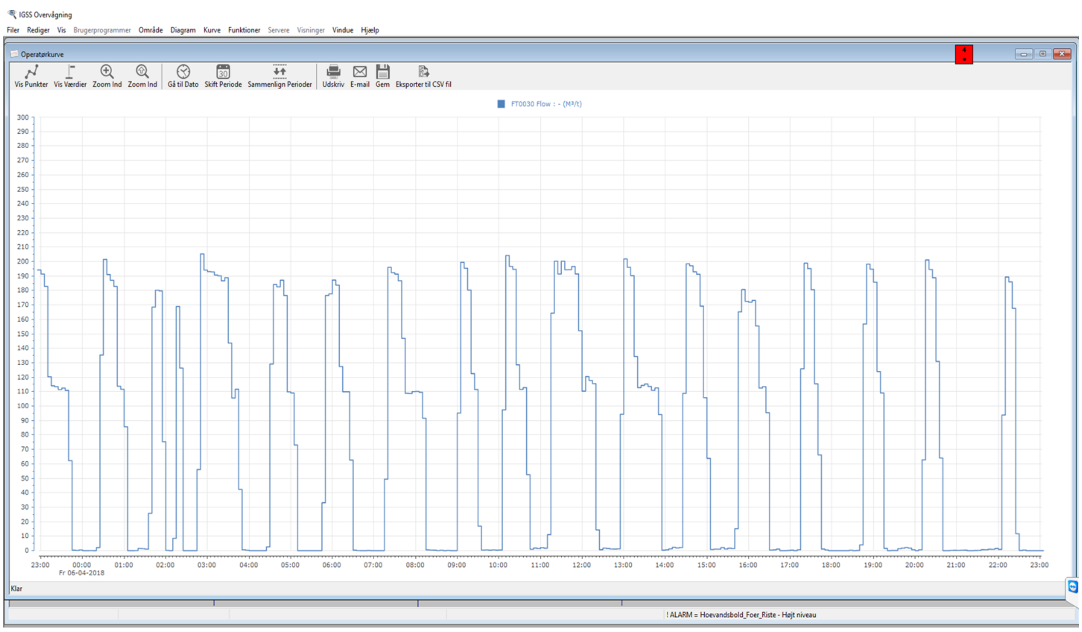

Figure 2.4: Flow profile from brewery and bottling plant combined during 24 hours.

From the figure it can be seen that the flow from industry is in pulses of up to 200 m^3/hr where the longest pulse is around an hour and the shortest is around 10 minutes. Between the pulse the flow is limited and the duration of these zones are must often around 30 minutes. From the plot it could seems like there are two pumps pumping the wastewater away from the industry, as there are two levels in the plot. Around 190-200 m^3/hr and around 110-120 m^3/hr. This data will be used to create the input to the main sewer line from the industry.

In figure 2.5 the flow input into the WWTP can be seen.

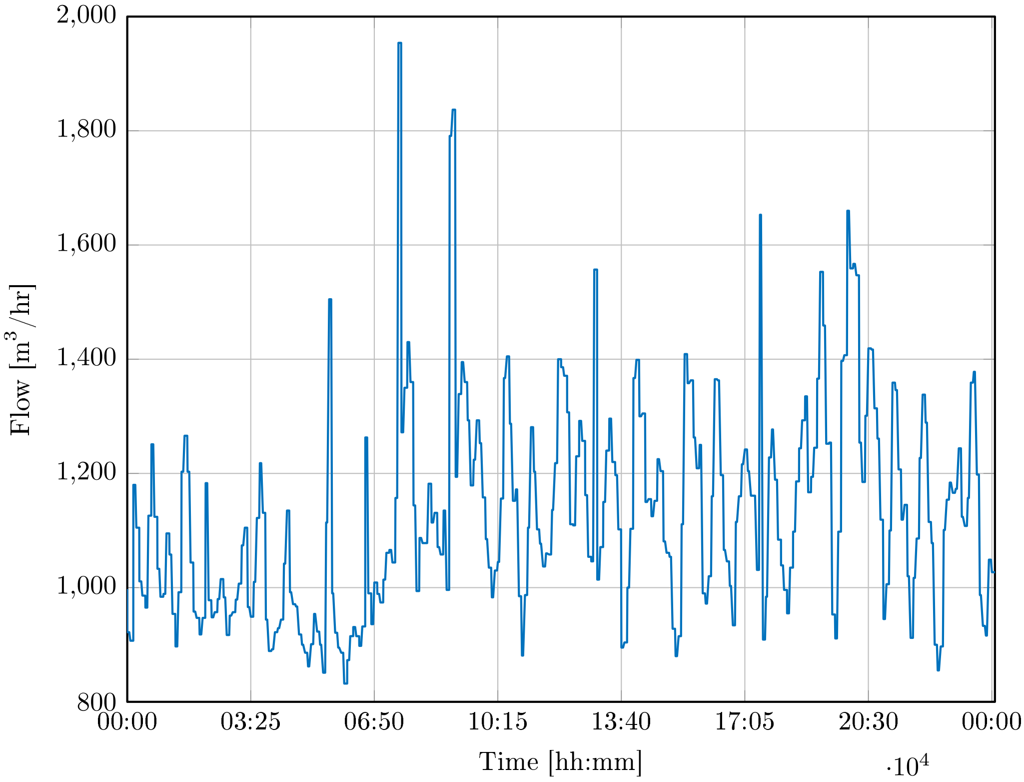

Figure 2.5: Flow input at Fredericia wastewater and treatment plant, from the fifth of February to the sixth of February.

From the figure, it can be seen how the flow into the WWTP fluctuates. From 00:00 to 03:25 the flow fluctuates between 1000 m^3/hr to 1200 m^3/hr and these huge shirts in flow rate is ongoing the entire day. Around 07:00 a large shift in flow occurs, it is unknown if this is a false measurement or it is due to a huge load change, as this peck seems to be only for one sample. However, it is very clear that the flow fluctuates across the entire day and it would be desirable to smooth the flow out.

In appendix ???? COD, phosphorus and nitrogen measurements from the input to the WWTP plan is shown. These figures show a similar pattern as the flow measurement, however, they do not vary as much as the flow. But a direct comparison cannot be done, as these measurements, the concentration measurements and the flow measurement, are measured at different dates, and therefore it can not be concluded if these concentrations are varying as much as the flow measurement. However, it can be concluded that these measurements also fluctuates across a day and therefore needs to be smoothed out to obtain a better cleansing process at the WWTP.

3 Simulation solutions & limitations

In this chapter different solutions will be discussed to find the most optimal solution to implement in Fredericia to limit the flow and concentration variations into the WWTP.

To limit the variations into the WWTP a mechanism is needed to hold back the wastewater. This could either be done by placing valves within the channels that would be able to limit the flow through a channel. This is done by opening or closing the valve and thereby the flow into the WWTP could be controlled. Another possibility is to store the wastewater in tanks and thereby control the output of the tank with e.g. a pump.

Using a valve to control/hold back the flow is correspond to using the pipe as a tank. In extreme cases, this could lead to overflow if not controlled properly and thereby cause wastewater to overflow into small rivers and other safety measures. However, it would be easier to install valves throughout the sewer network in respect to dig a large hole for a tank in the city. But after the meeting with the people from Fredericia Spildevand og Energi A/S it was stated that it would not be possible to use the sewer as a storing device as the sewer would be filled up to rapidly.

In this project, it is therefore decided to use a tank to limit the flow and concentration variation into the WWTP. Using a tank will remove these fluctuations, as seen in figure 2.5 for flow, by controlling the output of the tank properly, thus having an input to the WWTP that is less disrupted by variations. The output of the tank can be controlled to achieve a desired input to the WWTP, however, the tank must be controlled in a way where overflow in the tank is not permitted. The output of the tank can either be controlled by a pump or a valve, depended on the geographical location on the tank. In addition, from the meeting at Fredericia it was told, that in the case, where a tank was used as buffer in the system, it was needed to include retention time of the wastewater in the tank. The reason for this is, that if the wastewater is kept in the tank for a longer period, it will start to produces malodorous smells, due to the oxygen depletion, as the environment in the tank will go from an aerobic to an anaerobic environment.

Modeling 4

This chapter will in detail explain the modeling procedure of the various components comprising the sewer system seen in figure 2.1. In the following, methods to model the components such as flow in gravity and pressurized sewer lines (section 4.1), interconnections such that disturbances can be added to the main sewer line (section 4.2) and reservoirs in the sewer network (section 4.3). Furthermore transport of concentrate in the wastewater flowing in the main sewer line (section 4.4), is modeled.

4.1 Hydraulics of sewer line

A method to model hydraulics of gravity and pressurized sewer lines is explained respectively in the following.

4.1.1 Open channel

Modeling fluids is almost always done by considering it as a control volume. The reason is that it is rarely efficient, computational wise, or possible to consider the individual fluid particles. Henceforth the control volume will be denoted by the letter Ω which will correspond to some amount of fluid in a length of sewer line.

The open channel flow in gravity sewer lines can be described by the Saint-Venant equations which gives an expression for conservation of mass and momentum. Some assumptions is made when deriving the Saint-Venant equations [Schütze et al., 2011]:

1. The flow in the channel is one dimensional, and prismatic, and as such any curvature or change in width of the sewer line is considered negligible.
2. Fluid in the sewer line is considered incompressible.
3. The pressure is assumed hydrostatic.
4. The only forces considered is friction, pressure and gravity.
5. The water height and velocity is uniform in the cross-section and only changes horizontally i.e. turbulence in the fluid is not considered.
6. The slope of the channel bed is small

Continuity equation for conservation of mass gives an expression for the amount of fluid flowing into and out of the control volume plus the fluid stored in it. In figure 4.1 a flow in a channel is shown.

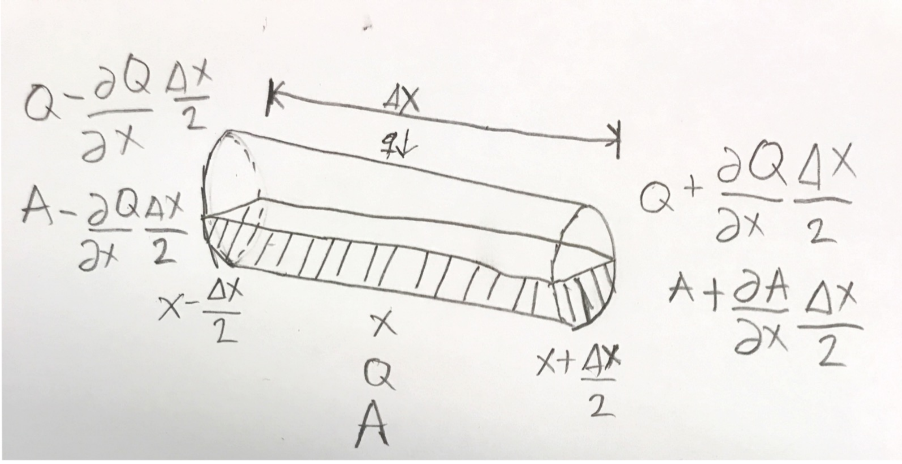

Figure 4.1: Illustration of a control volume, Ω, of fluid in a sewer pipe, where Q is flow into the end of the channel, q is lateral flow into the channel and A is the cross section area of the flow.

The flows and the cross section area of the flow, seen in figure 4.1, is dependent on time and position. In the following a simpler notation is used for an easier outline.

Flow into the control volume, where Q is the flow considered from the middle of the control volume, is given as:

$$Q_{in} \cdot \Delta t = \left(Q - \frac{\partial Q}{\partial x} \cdot \frac{\Delta x}{2} \right) \cdot \Delta t + q \cdot \Delta x \cdot \Delta t \tag{4.1}$$

Where q is lateral inflow across the entire channel $[\frac{m^2}{s}]$ and Q is the flow in the channel $[\frac{m^3}{s}]$. Lateral inflow could for example come from adjoint sewer pipes or road drain. The discharge flow of the channel is given as:

$$Q_{out} \cdot \Delta t = \left(Q + \frac{\partial Q}{\partial x} \frac{\Delta x}{2} \right) \cdot \Delta t \tag{4.2}$$

Average change in stored fluid in the channel is given as:

$$\begin{aligned} \frac{\partial}{\partial t} \left(\Delta x \cdot \frac{A - \frac{\partial A}{\partial x}\frac{\Delta x}{2} + A + \frac{\partial A}{\partial x}\frac{\Delta x}{2}}{2} \right) \Delta t &= \frac{\partial}{\partial t} \left(\Delta x \frac{2A}{2} \right) \Delta t \\ &= \frac{\partial A}{\partial t} \cdot \Delta x \Delta t \end{aligned} \tag{4.3}$$

As the flow into the channel minus the flow out is equal to the change in stored fluid in the channel, then due to the assumption of incompressible fluid and uniformity, the following can be written:

$$Q_{in} \cdot \Delta t - Q_{out} \cdot \Delta t = \frac{\partial A}{\partial t} \cdot \Delta x \cdot \Delta t \tag{4.4}$$

Inserting equations 4.1 and 4.2 in 4.4 the following is obtained:

$$\begin{aligned} &\left(Q - \tfrac{\partial Q}{\partial x} \cdot \tfrac{\Delta x}{2}\right) \cdot \Delta t + q \cdot \Delta x \cdot \Delta t - \left(Q + \tfrac{\partial Q}{\partial x} \tfrac{\Delta x}{2}\right) \cdot \Delta t = \tfrac{\partial A}{\partial t} \cdot \Delta t \cdot \Delta x \\ &\Updownarrow \\ &q \cdot \Delta x \cdot \Delta t - \tfrac{\partial Q}{\partial x} \cdot \Delta x \cdot \Delta t = \tfrac{\partial A}{\partial t} \cdot \Delta t \cdot \Delta x \end{aligned} \tag{4.5}$$

Equation 4.5 can be reduced to the following by isolating and dividing with Δx and Δt, on both sides, yielding the mass conservation part of the Saint-Venant equations.

$$\frac{\partial A(x,t)}{\partial t} + \frac{\partial Q(x,t)}{\partial x} = q(x,t) \tag{4.6}$$

For channel flows without lateral input the mass conservation is given as:

$$\boxed{\frac{\partial A(x,t)}{\partial t} + \frac{\partial Q(x,t)}{\partial x} = 0} \tag{4.7}$$

Momentum of the control volume Ω shown in figure 4.2 can be found by utilizing Newtons second law which states that force is equal to mass times acceleration. Basically this means that the momentum of the control volume can be found by integrating the sum of forces in the following differential equation:

$$\frac{d\mathcal{M}(t)}{dt} = \sum_i F_i(t) \tag{4.8}$$

Where $\mathcal{M}$(t) is the momentum, given as mass times a velocity vector, of the control volume at time t and F_i(t) is the various external forces affecting the control volume. The forces are given by the various hydrodynamic and hydrostatic effects which affects the control volume.

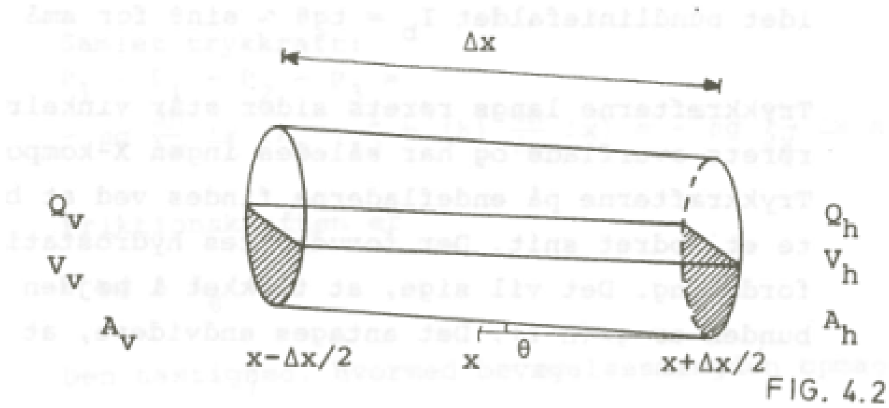

Figure 4.2: Illustration of the control volume Ω, .

If an infinite small slice of cross section in the control volume is considered, and utilizing the product rule on the hydrodynamic force acting on the slice, the following is obtained:

$$F = M \cdot \frac{dv}{dt} + \frac{dM}{dt} \cdot v \tag{4.9}$$

Due to the assumption of incompressible fluid in the control volume the mass derivative term in equation 4.9 can be rewritten to:

$$\frac{dM}{dt} = \rho\frac{dV}{dt} = \rho \cdot Q \tag{4.10}$$

If assuming static speed then the acceleration term can be neglected. Then by inserting equation 4.10 into equation 4.9 the force, given by the slice of fluid particles, can be written as:

$$F = \rho \cdot Q \cdot v \tag{4.11}$$

The hydrodynamic force given by the in- and output of fluid particles in the control volume, when considering a slice of fluid particles at the center of the control volume,is given as:

$$F_{in} = \rho \cdot v \cdot Q - \frac{\partial}{\partial x}(\rho \cdot v \cdot Q) \cdot \frac{\Delta x}{2} \tag{4.12}$$

$$F_{out} = \rho \cdot v \cdot Q + \frac{\partial}{\partial x}(\rho \cdot v \cdot Q) \cdot \frac{\Delta x}{2} \tag{4.13}$$

Where subscript "in" denote the force going in through the left side of the channel in figure 4.2 and subscript "out" is the force going out to the right side.The change of particle momentum in the control volume is given as $F_{in} - F_{out}$ and by replacing velocity with Q/A the following is obtained:

$$\underbrace{\rho \cdot \frac{Q}{A} \cdot Q - \frac{\partial}{\partial x}\left(\rho \cdot \frac{Q}{A} \cdot Q\right) \cdot \frac{\Delta x}{2}}_{F_{in}} - \underbrace{\left(\rho \cdot \frac{Q}{A} \cdot Q + \frac{\partial}{\partial x}\left(\rho \cdot \frac{Q}{A} \cdot Q\right) \cdot \frac{\Delta x}{2}\right)}_{F_{out}}$$
$$= -\rho\tfrac{\partial}{\partial x}\tfrac{Q^2}{A}\Delta x \tag{4.14}$$

The remaining to be found are the forces imposed by gravity, friction and pressure. The force applied by gravity is given as:

$$F_g = sin(\theta) \cdot g \cdot \rho \cdot \Delta x \cdot A \tag{4.15}$$

Where the slope of the pipe bed $\mathrm{S_b} = tan(\theta) \approx sin(\theta)$ for small values of θ yields:

$$F_g = S_b \cdot g \cdot \rho \cdot \Delta x \cdot A \tag{4.16}$$

The friction force can be set up as:

$$F_f = S_f \cdot g \cdot \rho \cdot \Delta x \cdot A \tag{4.17}$$

Where S_f is a friction coefficient. This coefficient can be estimated by different formulas like Manning's or Darcy-Weishbach formula which is seen in equation 4.18 and 4.19 respectively.

$$S_f = \frac{n^2Q^2}{A^2R^{4/3}} = \frac{n^2v^2}{R^{4/3}} \tag{4.18}$$

$$S_f = \frac{fQ^2}{8gRA^2} = \frac{fv^2}{8gR} \tag{4.19}$$

Where n is Manning's roughness factor $[\frac{s}{m^{1/3}}]$, f is the Weisbach resistance coefficient $[\cdot]$ and R is the hydraulic radius $[m]$ given as the wetted area divided by the wetted perimeter [Mays, 2001]. The Weisbach resistance coefficient is found by the Colebrook-White formula seen in equation 4.20.

$$\frac{1}{\sqrt{f}} = -2 \cdot log\left(\frac{k}{14.84 \cdot R} + \frac{2.52}{4Re\sqrt{f}}\right) \tag{4.20}$$

Where k is a pipe roughness coefficient and Re is the Reynolds number.

Last the pressure forces on the x component of the control volume to be found is shown as F_{P1}-F_{P3} in figure 4.3.

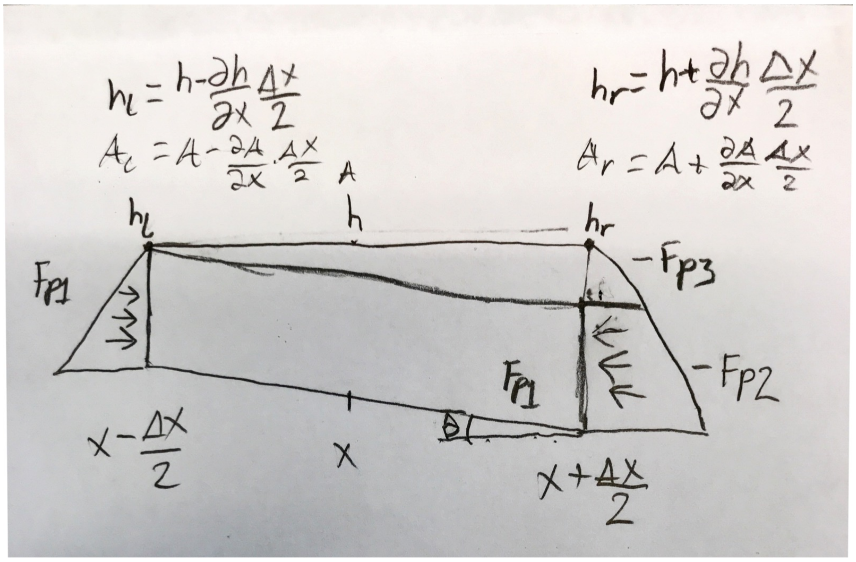

Figure 4.3: Pressure forces acting on the control volume

[1]

By assuming hydrostatic pressure, the pressure in a height, z, above the bottom of the channel is given as $g\rho(h-z)$, where h is the height of the fluid. The pressure force acting on the left side of the control volume is given as:

$$F_{P1} = \int_0^{h_l} \rho \cdot g(h_l - z) \cdot b(z)dz \tag{4.21}$$

Where h_l is the fluid height at the left side of the control volume, b(z) is the width of the channel given the height z. The force acting on the right side of the control volume is

[1] FiXme Note: Ny tegning og sikkert også caption

given as:

$$
\begin{aligned}
-\int_0^{h_r} \rho \cdot g \cdot (h_r - z) \cdot b(z)dz = &- \int_0^{h_l} \rho \cdot g \cdot (h_l - z) \cdot b(z)dz \\
&- \int_0^{h_l} \rho \cdot g \cdot (h_r - h_l) \cdot b(z)dz \\
&- \int_{h_l}^{h_r} \rho \cdot g \cdot (h_r - z) \cdot b(z)dz \\
=& - F_{P1} - F_{P2} - F_{P3}
\end{aligned} \tag{4.22}
$$

The pressure force acting on the right side, at a height h_l from the channel bed, is given by F_{P1}, F_{P2} and F_{P3} is the remaining force from h_l to h_r. The force F_{P2} is given as:

$$
\begin{aligned}
F_{P2} &= \int_0^{h_l} \rho \cdot g \cdot (h_r - h_l) \cdot b(z)dz \\
&= \int_0^{h_l} \rho \cdot g \cdot \left(h + \frac{1}{2}\frac{\partial h}{\partial x} - \left(h - \frac{1}{2}\frac{\partial h}{\partial x}\right)\right) \cdot b(z)dz \\
&= \rho g \frac{\partial h}{\partial x} \Delta x A_l
\end{aligned} \tag{4.23}
$$

The remaining pressure force, resulting from the height difference between h_l and h_r, is to be found. If, as a result of a small angle, it is assumed that the difference in height at each side is infinitely small. Then the force F_{P3} is given as:

$$
\begin{aligned}
F_{P3} &= \int_{h_l}^{h_r} \rho \cdot g \cdot (h_r - z) \cdot b(z)dz \\
&\approx \rho \cdot g \cdot b(h) \cdot \left[h_r \cdot z - \frac{z^2}{2}\right]_{h_l}^{h_r} \\
&= \rho \cdot g \cdot b(h) \cdot \left(h_r \cdot (h_r - h_l) + \frac{1}{2}\left(\frac{\partial h}{\partial x} \cdot \Delta x\right)^2\right) \\
&\approx \rho \cdot g \cdot b(h) \cdot \frac{1}{2}\left(\frac{\partial h}{\partial x}\Delta x\right)^2
\end{aligned} \tag{4.24}
$$

Taking the sum of forces from equations 4.21 and 4.22:

$$
\begin{aligned}
F_{P1} - F_{P1} - F_{P2} - F_{P3} = &- \rho g \frac{\partial h}{\partial x}\Delta x A_l - \rho g b(h) \frac{1}{2}\left(\frac{\partial h}{\partial x}\Delta x\right)^2 \\
=& - \rho \cdot g \cdot \frac{\partial h}{\partial x} \cdot \Delta x \left(A_l + \frac{1}{2} b(h) \frac{\partial h}{\partial x}\Delta x\right) \\
=& - \rho \cdot g \cdot \frac{\partial h}{\partial x} \cdot \Delta x \left(A_l + \frac{1}{2}\frac{\partial A}{\partial x}\Delta x\right) \\
=& - \rho \cdot g \cdot \frac{\partial h}{\partial x} \cdot \Delta x \cdot A
\end{aligned} \tag{4.25}
$$

By summing all the forces from equation 4.14, 4.15, 4.17 and 4.25 and inserting them into equation 4.8 the following is obtained:

$$\begin{aligned} -\sum_i F_i = &- \frac{\partial}{\partial x}\rho\frac{Q^2}{A}\Delta x \\ &- S_b \cdot g \cdot \rho \cdot \Delta x \cdot A \\ &- S_f \cdot g \cdot \rho \cdot \Delta x \cdot A \\ &- \rho \cdot g \cdot \frac{\partial h}{\partial x} \cdot \Delta x \cdot A \end{aligned} \tag{4.26}$$

Lastly the time derivative expression of the momentum, which is given by mass times velocity, are:

$$\frac{d\mathcal{M}(t)}{dt} = \frac{\partial}{\partial t}\left(\rho \cdot A \cdot \Delta x \cdot \frac{Q}{A}\right) \tag{4.27}$$

Where mass is given by $\rho \cdot A \cdot \Delta x$ and velocity by Q/A.

Having obtained expressions for equation 4.27 and equation 4.26 they can be inserted into equation 4.8 yielding the following expression:

$$\begin{aligned} \frac{\partial}{\partial t}(\rho\frac{Q}{A}A \cdot \Delta x) = &- \frac{\partial}{\partial x}\rho\frac{Q^2}{A}\Delta x \\ &- S_b \cdot g \cdot \rho \cdot \Delta x \cdot A \\ &- S_f \cdot g \cdot \rho \cdot \Delta x \cdot A \\ &- \rho \cdot g \cdot \frac{\partial h}{\partial x} \cdot \Delta x \cdot A \end{aligned} \tag{4.28}$$

Dividing with $g \cdot \rho \cdot \Delta x \cdot A$ and isolating, then the following definition of the equation is obtained:

$$\boxed{\frac{1}{gA}\frac{\partial Q}{\partial t} + \frac{1}{gA}\frac{\partial}{\partial x}\left(\frac{Q^2}{A}\right) + \frac{\partial h}{\partial x} + S_f - S_b = 0} \tag{4.29}$$

Some or all of the terms in equation 4.29 can be utilized when simulating free channel flow. An overview of the limitations when excluding parts of the momentum equation is given in table 4.1.

Approximation	Kinematic wave (1)	Noninertia (2)	Quasi-steady dynamic wave (3)	Dynamic wave (4)
momentum equation	$S_b = S_f$	$\frac{\partial h}{\partial x} = S_b - S_f$	$\frac{1}{gA}\frac{\partial}{\partial x}\left(\frac{Q^2}{A}\right) + \frac{\partial h}{\partial x}$ $= S_b - S_f$	equation 4.29
Boundary conditions required	1	2	2	2
Account for downstream backwater effect and flow reversal	No	Yes	Yes	Yes
Damping of flood peak	No	Yes	Yes	Yes
Account for flow acceleration	No	No	only convective acceleration	Yes

Table 4.1: Limitations when excluding, 1.(inertia and pressure terms), 2.(inertia terms), 3.(pressure term relating to local acceleration) and 4.(none), from the momentum equation [Mays, 2001].

The kinematic wave is the simplest approximation and ignores the terms representing changes in inertia and pressure by assuming that the slope of the water surface is identical to that of the channel bed. Furthermore only one boundary condition is needed, meaning that only the upper boundary of the channel is needed to solve the Saint-Venant equations. Some considerations is needed when utilizing this approximation. Due to the simplicity of the kinematic wave approximation, attenuation, which occurs in a real free flowing channel, should not be present. But due to numerical damping, which is induced because of the nature of discretization, it occurs. Some, wrongfully attempts to mitigate it by choosing smaller steps of Δx and Δt. Instead they should be chosen such that the simulated channel flow mimics that of the real channel. Due to its simplicity the kinematic wave approximation has been used and researched extensively. If the back water effect is not an issue the kinematic wave approximation is often used when dealing with simulation of flows in sewer lines. To limit the complexity of the further work of the project, the kinematic wave approximation, of the momentum equation, is chosen [Mays, 2001]. Furthermore it is decided to disregard lateral input, i.e. not take gutter drains into consideration. This means that side input to the main sewer line is assumed attached at the end of the pipe section as shown in table 2.1. Further details can be found in section 4.2.

4.1.2 Pipe model

When the wastewater requires to be elevated from lower geographical point to another it is done using a pump connected with pipes to lead the wastewater to a higher point. Therefore a model of a pipe is needed to describe the flow change within this pipe. Therefore in this subsection a model for a pipe will be elaborated.

In figure 4.4 an illustration of a pipe is shown.

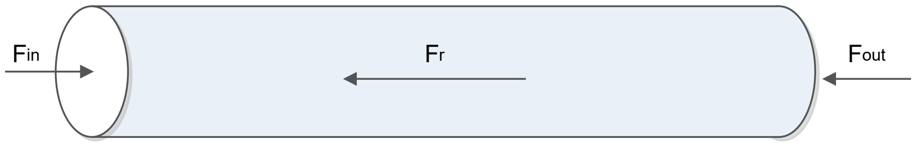

Figure 4.4: Illustrate the forces within a pipe.

Where the three forces shown in figure 4.4, F_{in}, F_r and F_{out}. F_{in} is the force going into the pipe, F_r is the resistance force within the pipe, such as pipe wall and bends. And lastly F_{out} which is the force going out of the pipe. These forces are effecting the wastewater inside the pipe and is equal to the rate of change in the momentum of the fluid.

$$\frac{d\mathcal{M}}{dt} = F_{sum} \tag{4.30}$$

Where $\mathcal{M}$ is the momentum $\left[\frac{kg \cdot m}{s}\right]$ and F_{sum} is the sum of all the forces $[N]$. Assuming that the fluid is incompressible and the pipe is filled with wastewater the following can be obtained:

$$\frac{d\mathcal{M}}{dt} = \frac{d(M \cdot v)}{dt} = M\frac{dv}{dt} = F_{sum} \tag{4.31}$$

Where M is the mass of the fluid $[kg]$ and v is the velocity $\left[\frac{m}{s}\right]$. The mass of the fluid can be written as density times the volume of the pipe,

$$M = \rho \cdot V \tag{4.32}$$

Where ρ is the density of liquid $\left[\frac{kg}{m^3}\right]$ and V the volume of the pipe $\left[m^3\right]$. Assuming the pipe is a cylinder, with a constant cross-sectional area along the pipe, the volume of the pipe can be written as,

$$V = A \cdot l \tag{4.33}$$

Where A is the area of a circle $[m^2]$ and l is the length of the pipe [m]. Inserting the previous expressions in equation 4.31 the following is obtained,

$$\rho \cdot A \cdot l \cdot \frac{d}{dt}v = F_{in} - F_{out} - F_r \tag{4.34}$$

The velocity of the fluid is written as,

$$v = \frac{Q}{A} \tag{4.35}$$

Where Q is the flow through the pipeline $\left[\frac{m^3}{s}\right]$.

The input, output and resistance force are written as $F = p \cdot A$, where p is the pressure [Pa]. Inserting the expression in 4.34 the following is obtained,

$$\rho \cdot A \cdot l \cdot \frac{d}{dt}\left(\frac{Q}{A}\right) = p_{in} \cdot A - p_{out} \cdot A - p_r \cdot A \tag{4.36}$$

Simplified to,

$$\frac{\rho \cdot l}{A} \cdot \frac{d}{dt}Q = \Delta p - p_r \tag{4.37}$$

Where the pressure difference is expressed as Δp and the area is divided on both sides.

The resistance pressure can now be divided into two resistance, namely form resistance and surface resistance [Prabhata K. Swamee, 2008].

Surface resistance:
The surface resistance describes the pressure loss across a straight pipe [Prabhata K. Swamee, 2008].

$$h_f = \frac{8 \cdot f \cdot l}{\pi^2 \cdot g \cdot d^5} \cdot |Q| \cdot Q \tag{4.38}$$

Where h_f is the head loss for the surface resistance of the pipe $[m]$, f is a coefficient for surface resistance, also knows as the friction factor, g is the gravitational acceleration $\left[\frac{m}{s^2}\right]$ and d is the diameter of a circular pipe $[m]$.

Form resistance:
The form resistance describes the pressure losses from fittings in a hydraulic network [Prabhata K. Swamee, 2008].

$$h_l = k_L \frac{|v| \cdot v}{2 \cdot g} \tag{4.39}$$

Where h_l is the head loss for the form resistance of the pipe [m] and k_L is the form-loss coefficient. The form-loss coefficient varies for different components e.g. threaded elbows and tees. The coefficient for the different components can be found in [Munson et al., 1998].

The pressure resistance in the pipe is expressed as:

$$p_r = \rho \cdot g \cdot h_n \tag{4.40}$$

Where h_n are the surface and form resistance. Besides these resistance, there is also a pressure resistance due to elevation between the two ends of a pipe. This is given as $\Delta z g \rho$ which is also known as the hydrostatic force. Where Δz is the height difference. By substituting p_r in equation 4.37 with equation 4.40 the following is obtained:

$$\frac{\rho \cdot l}{A} \cdot \frac{d}{dt}Q = \Delta p - \rho \cdot g \cdot h_n \tag{4.41}$$

The surface and form, equations 4.38, 4.39 and the hydrostatic force can be inserted into equation 4.41:

$$\frac{\rho \cdot l}{A} \cdot \frac{d}{dt}Q = \Delta p - \rho \cdot g \left(k_L \frac{|v| \cdot v}{2 \cdot g} + \frac{8 \cdot f \cdot l}{\pi^2 \cdot g \cdot d^5} \cdot |Q| \cdot Q + \Delta z \right) \tag{4.42}$$

Substitute the head loss factors with k_v, a coefficient describing the pressure losses in the pipes, and $\frac{\rho \cdot l}{A}$ is inertance J. The final pipe model is expressed as:

$$\boxed{J \cdot \frac{d}{dt} Q = \Delta p - \rho \cdot g \cdot k_v} \tag{4.43}$$

4.1.3 Pump model

In this section a model of a pump will be elaborated. The model for the pump will be used in the simulation to rise the wastewater from a lower position to a higher one.

The model for a pump is expressed as [Kallesøe, 2005].

$$\Delta p = (-a_{n2} Q^2 + a_{n1} Q\omega + a_{n0}\omega^2)\rho g \tag{4.44}$$

Where a_{n2}, a_{n1} and a_{n0} are the constant parameters of the pump, Q is the flow of the water $\frac{m^3}{s}$, $[\omega]$ is the angular velocity of the pump $[\frac{rad}{s}]$ and p is the pressure delivered by the pump [Pa]. In table 4.2 the parameters for the pump can be found. [2]

Parameters:	a_{n2}	a_{n1}	a_{n0}
Values:	-0,1830	-1,8004	7,0579

Table 4.2: Parameters for the pump model [Kallesøe, 2005].

4.2 Sewer interconnection

This section will explain how interconnection between channels are modeled and how the mixing between wastewater and wastewater with chemicals.

In figure 4.5 an illustration of a interconnection between two flows are shown.

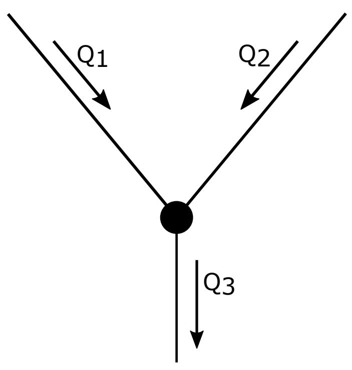

Figure 4.5: Illustration of an interconnection between two flow inputs and one output.

[2] FiXme Note: Enten skal vi slette den her tabel, eller os skal vi have fundet nogle andre pumpe parameter.

[3]

The two channels Q_1 and Q_2 are connected at the end of each channel here the wastewater from the two channels will be added up. The flow Q_3 is calculated as:

$$Q_3 = Q_1 + Q_2 \tag{4.45}$$

For the mixing between two flows where one of them is transporting chemicals will be done in similar way as for flows.

$$C_3 = \frac{C_1 Q_1 + C_2 Q_2}{Q_3} \tag{4.46}$$

Where C is the amount of chemicals $[\frac{g}{m^3}]$. This is done to keep the same amount of chemicals within the wastewater, as the algorithm for transporting chemicals is depended on flow, as seen in section 4.4. If it is not calculated like this, thus when the flow is increasing the same will the chemicals within the wastewater, hence it is needed to divided by Q_3 to get the right amount of chemicals in the wastewater.

4.3 Sewer reservoir

In this section the model for a reservior will be derived. The assumptions made deriving the tank model is:

1. The pressure is considerede hydrostatic.

In figure 4.6 an illustration of a reservoir is shown.

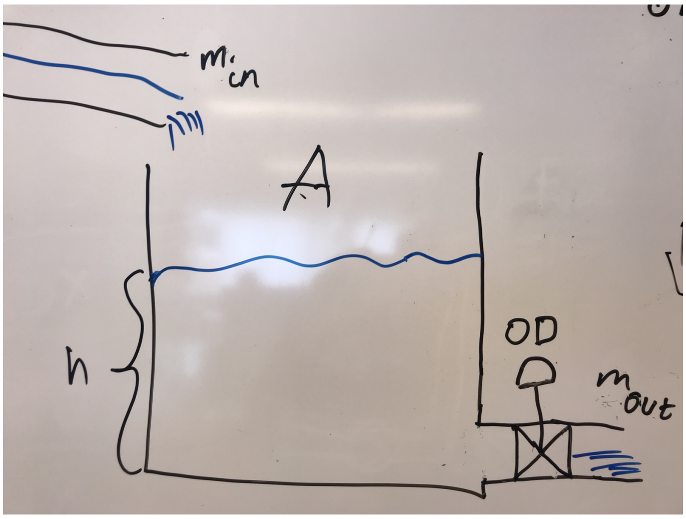

Figure 4.6: An illustration of a reservoir.

[3] FiXme Note: Ny tegning

This illustration will be used to derive the model for the reservior. From the left an open channel that discharges fluid into the reservoir is shown. The fluid going into the reservoir has a mass flow rate, m_{in} $[\frac{kg}{s}]$. Within the reservoir the stored fluid has a height, h $[m]$, and the reservoir has a surface area, A. To the bottom right the fluid is discharged, m_{out}. The output mass flow is depended on the openings degree (OD) of the valve. The mass balance equation is derived in [Vojtesek et al.,] and is given as:

$$\frac{dM_{cv}(t)}{dt} = m_{in}(t) - m_{out}(t) \tag{4.47}$$

Where M_{cv} is the total mass within the control volume $[kg]$, and m_{in} and m_{out} is the mass in and outflow rate of the tank $\left[\frac{kg}{s}\right]$. The mass balance can be written as $M_{cv} = \rho Ah$ where ρ is the densisty $\left[\frac{kg}{m^3}\right]$, A is the area $\left[m^2\right]$ and h is the height [m]. The mass flow rate can be written as $m = \rho Q$, where Q is the flow $\left[\frac{m^3}{s}\right]$. Inserting this into equation 4.47 the following is obtained:

$$\frac{d(\rho Ah(t))}{dt} = \rho Q_{in}(t) - \rho Q_{out}(t) \tag{4.48}$$

By assuming incompressible fluid such that density is constant then:

$$\rho A\frac{dh(t)}{dt} = \rho\left(Q_{in}(t) - Q_{out}(t)\right) \tag{4.49}$$

Simplifying equation 4.49 by dividing with ρA:

$$\frac{dh(t)}{dt} = \frac{1}{A}\left(Q_{in}(t) - Q_{out}(t)\right) \tag{4.50}$$

Because the output flow is depending on the OD of the valve, a model is needed to described the output flow of it. The model for the valve is derived by [Boysen, 2011] and is given as:

$$Q_{out} = kv(OD)\sqrt{\Delta p} \tag{4.51}$$

Where kv(OD) is a function that describes the flow for different ODs. Δp is the pressure drop across the valve [Pa]. The pressure difference across the valve is the pressure at the bottom of the tank minus the pressure in the open channel. The pressure at the bottom of the tank can be found with: [4]

$$P_{bot} = P_{top} + \rho gh \tag{4.52}$$

Where P_{top} is the atmospheric pressure $[Pa]$ and g is the gravitational constant $\left[\frac{m}{s^2}\right]$. The pressure on the output side of the valve is assumed to be 1 atm as it is an open channel. Inserting equation 4.52 into equation 4.51 the following is obtained:

$$Q_{out} = kv(OD)\sqrt{(P_0 + \rho gh) - P_0} = kv(OD)\sqrt{\rho gh} \tag{4.53}$$

[4] FiXme Note: Skal nok jhave noget med ventil karakterstik med

Equation 4.53 can be inserted into equation 4.50 and thereby the following model for the reservoir is obtained.

$$\frac{dh(t)}{dt} = \frac{1}{A}\left(Q_{in}(t) - \left(kv(OD)\sqrt{\rho g h(t)}\right)\right) \tag{4.54}$$

Equation 4.54 then gives an expresion where change in height is given as a function of inflow, pressure and opening degree of the valve.

4.4 Transport of concentrate

A model for transport of concentrate in sewer pipes is obtained in the following. The following assumptions is made obtaining the transport equation.

1. The flow of concentrate is assumed to be steady and uniform in the cross section.
2. The anoxic, anaerobic or aerobic processes occurring in the sewer line is neglected

In figure 4.7 a control volume is seen.

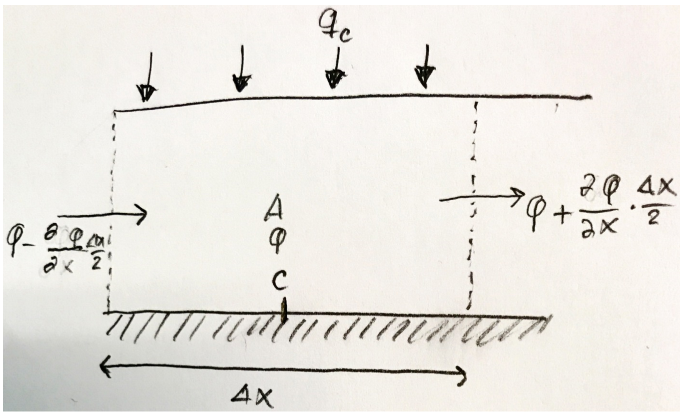

Figure 4.7: Illustration of a control volume containing concentrate.

The conservation of concentrate in the control volume is as in section 4.1 dependent on the change in stored mass and change in flow. This means that the equation for conservation of mass given by equation 4.6, which is shown below, can be utilized.

$$\frac{\partial A}{\partial t} + \frac{\partial Q}{\partial x} = q \tag{4.55}$$

Assuming average concentrate, C, across the control volume, and multiplying it with the terms of the continuity equation, the following is obtained:

$$\frac{\partial A \cdot C}{\partial t} + \frac{\partial \phi}{\partial x} = q \cdot C_{lat} \tag{4.56}$$

Where ϕ is a flux $[\frac{g}{s}]$ term replacing the flow term, Q and C_{lat} is lateral concentrate input into the control volume $[\frac{g}{m^3}]$ [Vestergaard, 1989].

Depending on the desired approximation the flux and lateral inflow terms can be expanded. The expanded lateral term describes a dead zone at the bottom of the channel, which can be useful to model if dealing with rugged channel bed. Due to the prismatic assumption in 4.1 of the sewer channel the dead zone in the channel is not investigated further. Flux terms describing convective flow and dispersion can be seen in table 4.3.

Approximation	Convective flow	Convective + (dispersion)
Flux term	$\phi = Q \cdot C$	$\phi = Q \cdot C + \left(-\epsilon \cdot A \frac{\partial C}{\partial x}\right)$
boundary conditions required	1	2

Table 4.3: Table of convective flux term without and with dispersion where Q is flow, C is concentrate, A is area and ϵ is a dispersion coefficient $[\frac{m^2}{s}]$ [Vestergaard, 1989] .

The dispersion term shown in the above table, also known as Fickian diffusion, gives an expression for how the molecules of the concentrate spreads. On a molecular level the the concentrate will to some degree disperse upstream and downstream as shown in figure 4.8.

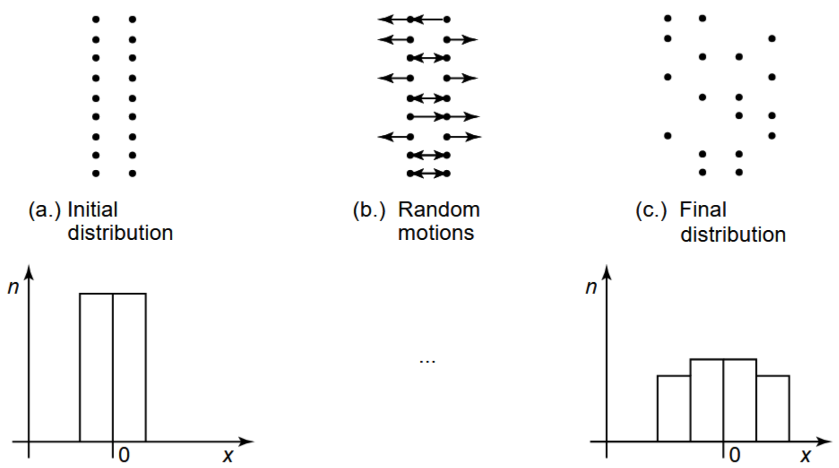

Figure 4.8: Illustration of distribution of convective flow without dispersion (a) and with (c), where dots illustrate molecules of the concentrate within a control volume [Institue of hydromechanics,].

For various concentrates the dispersion coefficient ϵ which varies with temperature can be found in lookup tables [Institue of hydromechanics,].

Inserting the terms in table 4.3 into equation 4.56 then the following expressions of the continuity equation is obtained:

$$\frac{\partial(A \cdot C)}{\partial t} + \frac{\partial(Q \cdot C)}{\partial x} - \epsilon \cdot \frac{\partial^2(A \cdot C)}{\partial x^2} = q \cdot C_{lat} \tag{4.57}$$

$$\frac{\partial(A \cdot C)}{\partial t} + \frac{\partial(Q \cdot C)}{\partial x} = q \cdot C_{lat} \tag{4.58}$$

In closed environments such as sewers longitudinal dispersion can often be neglected [Vestergaard, 1989]. For this reason and to reduce complexity of the simulation, equation

4.58 is utilized further on. As the change in flow and area in the channel is solved by the Saint-Venant equations, an expression which only considers change in concentrate suffices. The terms in equation 4.58 can be rewritten to the following:

$$C \cdot \frac{\partial A}{\partial t} + A \cdot \frac{\partial C}{\partial t} + C \cdot \frac{\partial Q}{\partial x} + Q \cdot \frac{\partial C}{\partial x} = q \cdot C_{lat} \tag{4.59}$$

Multiplying equation 4.55 with C yields:

$$C \cdot \frac{\partial A}{\partial t} + C \cdot \frac{\partial Q}{\partial x} = q \cdot C \tag{4.60}$$

Subtracting equation 4.60 from 4.59 then results in the following:

$$A \cdot \frac{\partial C}{\partial t} + Q \cdot \frac{\partial C}{\partial x} = q \cdot (C_{lat} - C) \tag{4.61}$$

Neglecting lateral flow and concentration inputs the following expression is obtained:

$$\boxed{A \cdot \frac{\partial C}{\partial t} + Q \cdot \frac{\partial C}{\partial x} = 0} \tag{4.62}$$

Equation 4.62 can thereby be solved with the solutions of Q and A obtained from the Saint-Venant equations.

Simulation 5

In this chapter, an overview is given of the design process of the simulation environment. Furthermore, the schemes utilized to be able to simulate the nonlinear parts of the sewage flow, with its various concentrations, is explained. Lastly, the designed environment is implemented and verified. It is decided to utilize MATLAB as the platform to be used for this project. Furthermore, it is assumed that readers are familiar with basic terminology related to MATLAB, and therefore specifics will not be given hereof.

In the following, the basic structure of the simulation and the design of it is explained.

5.1 Structure

For the simulation environment to be useful, some basic functionality is needed. The simulation should be easy to setup and adjust if needed. Furthermore, an easy way to view the result of the simulation is needed such that necessary adjustments can easily be made based on the result.

The first overall thing to consider is the composition of components desired to simulate. To make the simulation environment useful it should be able to handle different compositions of pipes and tanks. Meaning that the simulation environment can simulate different setups than the one shown in figure 2.1. For this, a simple setup procedure, where different sizes of pipes with different parameters can be chosen, is needed. The second thing to consider is that the environment should be brought to a steady state before the simulation starts. The reason for this is that unintended results can arise when working with non-linear systems. Also if a linearized approach to the MPC scheme is chosen a linearized model is necessary, which requires a system in steady state to obtain. The simulation should be able to run for a predefined amount of iterations. Based on this the basic structure of the simulation environment can be split into three parts as shown in figure 5.1.

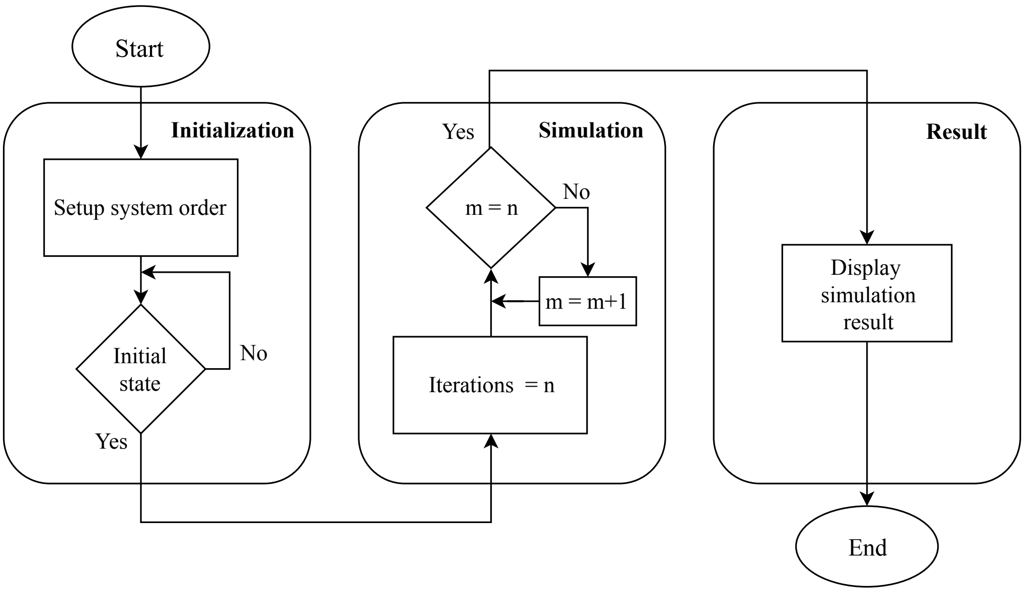

Figure 5.1: Basic overview of simulation environment

The following will go into details, on the thoughts and the considerations made during the design phase, of the three parts shown in the figure.

Initialization

The initialization process is, as shown in figure 5.1, comprised of several parts. The first part is to set up the desired system of pipes and tanks such that the system is simulated with the chosen components in the right order. Secondly, the system should be brought in to a steady state from which the simulation can start. The reason for this is that the Saint-Venant equations utilized to simulate the flow in the sewer pipes is non-linear. Because of this, it can be difficult to find a steady state by hand, which do not produce an unintended result when starting simulating. Though it might be possible to find fitting initial values for small setup it is assumed that larger setup will increase the chance of unintended results when starting simulating.

For the first part, a simple system setup is decided upon, where the desired components are added to a list. The order of the list then decides how the components is connected when simulating. An example of this setup procedure is shown in figure 5.2.

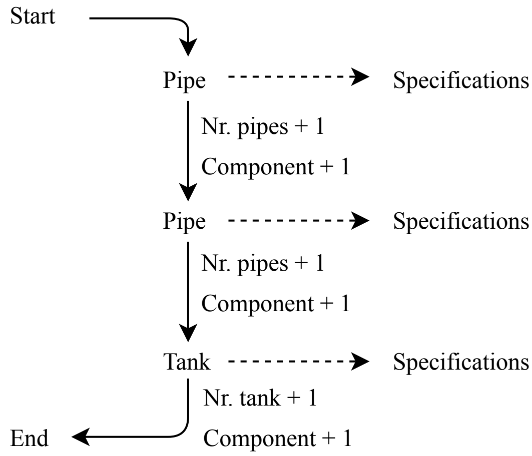

Figure 5.2: Setup scheme of system order initiation

The specifications for each part in figure 5.2 refers to the parameters needed to run the simulation. The necessary specifications entered for pipe and tank should as a minimum be the required parameters needed to utilize the Preissmann scheme explained in section 5.2 and to simulate in- and outflow of one or more tanks, respectively. Furthermore, constants which are utilized during simulation should be calculated during initialization such that the computational load is kept as low as possible during simulation.

A simple solution to bring the desired system setup to an initial steady state is to give a fixed input flow and iterate. The iteration continues until a satisfactory error between the fixed input and the flow within the designated setup is deemed sufficiently low. For this to work, it is important to have side input or disturbance input in mind. In figure 5.3 a simple setup is shown of a possible setup to be simulated.

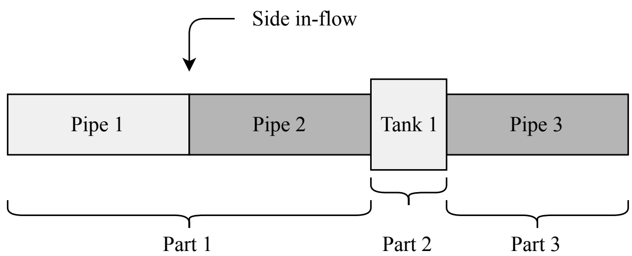

Figure 5.3: Simple setup with three pipes, a tank and a single side input

To make the steady state iteration scheme work on a dynamic level, the components can be separated into parts where adjoint pipes are seen as a single part. The system can then be brought in to steady state one part at a time. As the pipes are the only non-linear part of the system, they are the only parts needed to be iterated upon. Taking the first part in figure 5.3 as an example, there are two pipes and the second one has a side input. A general expression of the average flow in the parts containing pipes is given by the following equation:

$$\text{Part-m}_{\text{avg}} = \frac{\sum_{i=1}^{n} \text{Pipe-input}_i + \text{side inflow}_i}{n_{\text{pipes}}} \tag{5.1}$$

Equation 5.1 can then be used to obtain the desired steady state flow and a current one by utilizing values obtained by solving the Saint-Venant equations. The iteration can then be set to stop when the error between the desired and the measured average is sufficiently low. The next part in figure 5.3 is, in this case, a tank, set to have an in- and outflow equal to the output of the second pipe, which is the combined flow of the first pipe plus the side input. For the third part, the iteration process then starts over with the outflow of the tank as input. As the concentrate flow is depending on the solution of the Saint-Venant equations it is assumed that when the flow is in a steady state the concentrate will have reached steady state as well.

Simulation

Having obtained a setup in steady state the next part is to simulate it for the predefined amount of iterations. An important part of the simulation is to store data in a way such that it is easily and intuitively obtainable for purposes such as debugging or customized plots. For this reason, it is decided to store the data, from simulating, into separate blocks. This means that data from individual pipes and tanks should be stored separately in the order given by the initial component setup shown in figure 5.2. In figure 5.4 a simple overview of the simulation procedure is given.

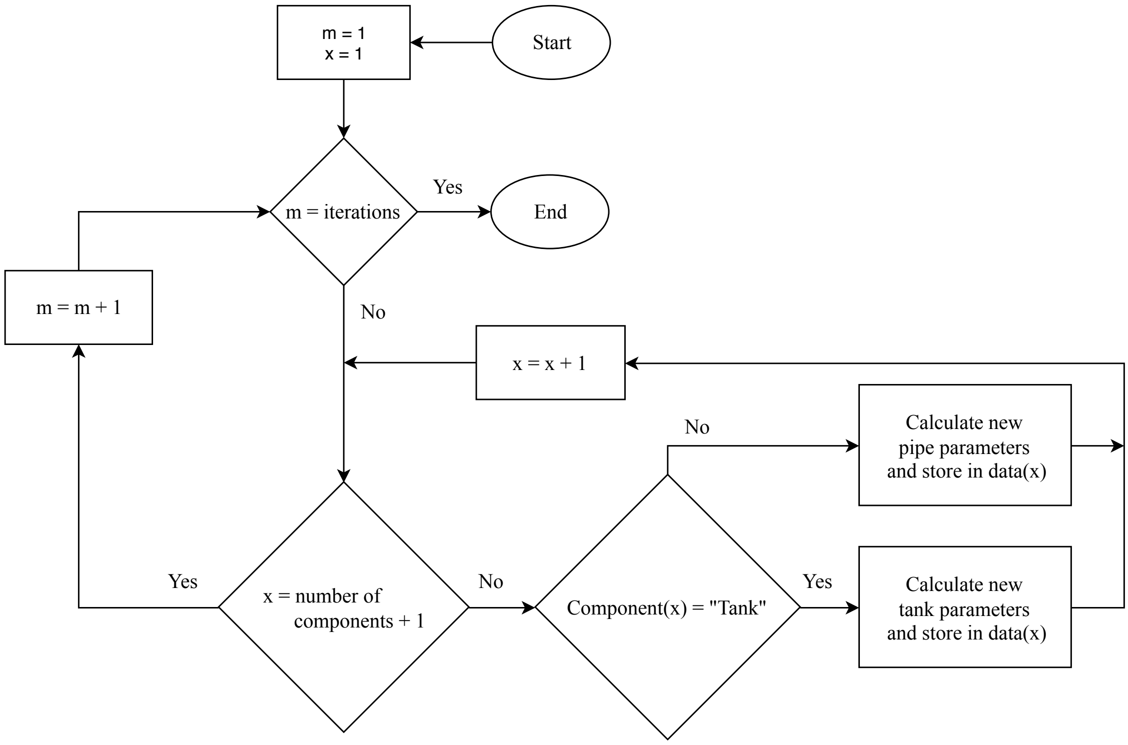

Figure 5.4: Basic overview of the simulation scheme.

Result

Having obtained data from simulating the user-defined system an overview of the results is needed. Considerable time can be spent in designing a function which can display the data in various forms. As the data can consist of a large number of components as well as a considerable time span it can get quite time-consuming to pinpoint parts of interest in time and place. For this reason, it is decided that a simple solution which can give an overview, of the obtained data, is needed. The chosen solution is a function which can playback the simulated data at a user defined speed and intervals in the data. Furthermore, it should be possible to pause and start the playback at a user-defined iteration.

Having outlined the basic details of the construction of the simulation environment the scheme needed to solve the non-linear Saint-Venant equations is explained in detail in the next section.

5.2 Preissmann scheme

In this section, the Saint Venant equations are solved using a numerical method.

The numerical method used for solving the Saint Venant equations, described in section 4.1, is the Preissmann scheme which is based on the box scheme. Other methods exist such as Lax scheme, Abbot-Ionescu scheme, leap-frog scheme, Vasiliev scheme, however, the Preissmann scheme is commonly known as the most robust. Basically, by using the Preissmann scheme the Saint Venant equations can be discretized, and thereby utilized to simulate the flow and height throughout an open channel.

From section 4.1 the Saint Venant equations for conservation of mass and momentum are derived, they are also shown below.

$$\frac{\partial A(x,t)}{\partial t} + \frac{\partial Q(x,t)}{\partial x} = 0 \tag{5.2}$$

$$\frac{1}{gA}\frac{\partial Q}{\partial t} + \frac{1}{gA}\frac{\partial}{\partial x}\left(\frac{Q^2}{A}\right) + \frac{\partial h}{\partial x} + S_f - S_b = 0 \tag{5.3}$$

In figure 5.5 a single mesh for the Preissmann scheme is illustrated.

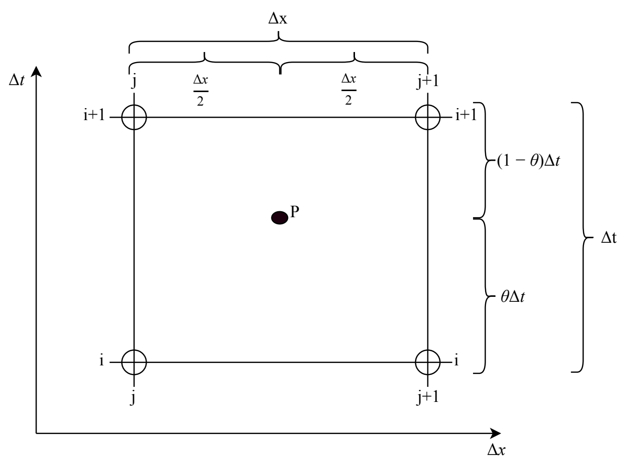

Figure 5.5: Preissmann non-staggered grid scheme.

Where θ is a weighting parameter ranging between zero and one, j is an index of cross section and i is an index of time. The mesh contains four nodes, (j,i), (j+1,i), (j,i+1) and (j+1,i+1), however in the implementation the dimension of the grid is $\Delta t \times \Delta x$ for $0 \leq x \leq L$ and $0 \leq t$. Where L defines the length of the open channel section. The derivatives in equations 5.2 and 5.3 are calculated as an approximation at the point P, which is in the middle of the interval of Δx.The difference between the box scheme and the Preissmann scheme is that the point P is always found at the middle of Δx and the point can only move along the time axis within this mesh by adjusting the weighting parameter θ. This weighting parameter will be elaborated on later. An arbitrary function $f_p(x,t)$ calculated at point P is approximated by [Szymkiewiczi, 1998].

$$f_P \approx \frac{1}{2}(\theta \cdot f_j^{i+1} + (1-\theta) f_j^i) + \frac{1}{2}(\theta \cdot f_{j+1}^{i+1} + (1-\theta) f_{j+1}^i) \tag{5.4}$$

The numerical approximation for the derivatives in equations 5.2 and 5.3 for time and length are shown below [Szymkiewiczi, 1998].

$$\left.\frac{\partial f}{\partial t}\right|_P \approx \frac{1}{2}\left(\frac{f_j^{i+1} - f_j^i}{\Delta t} + \frac{f_{j+1}^{i+1} - f_{j+1}^i}{\Delta t}\right) \tag{5.5}$$

$$\left.\frac{\partial f}{\partial x}\right|_P \approx (1-\theta)\frac{f_{j+1}^i - f_j^i}{\Delta x} + \theta\frac{f_{j+1}^{i+1} - f_j^{i+1}}{\Delta x} \tag{5.6}$$

These approximations from equations 5.5 and 5.6 can therefore be inserted for the derivatives in the Saint Venant equations 5.2 and 5.3 and thereby achieve the following,

$$\theta\frac{Q_{j+1}^{i+1} - Q_j^{i+1}}{\Delta x} + (1-\theta)\frac{Q_{j+1}^i - Q_j^i}{\Delta x} + \frac{1}{2}\frac{A_{j+1}^{i+1} - A_{j+1}^i}{\Delta t} + \frac{1}{2}\frac{A_j^{i+1} - A_j^i}{\Delta t} = 0 \tag{5.7}$$

$$\frac{1}{gA_p}\left(\frac{1}{2}\left(\frac{Q_{j+1}^{i+1}-Q_{j+1}^{i}}{\Delta t}+\frac{Q_{j}^{i+1}-Q_{j}^{i}}{\Delta t}\right)\right)+\frac{1}{gA_p}\left(\frac{\theta}{\Delta x}\left(\left(\frac{Q^2}{A}\right)_{j+1}^{i+1}-\left(\frac{Q^2}{A}\right)_{j}^{i+1}\right)\right)+$$
$$\frac{1-\theta}{\Delta x}\left(\left(\frac{Q^2}{A}\right)_{j+1}^{i}-\left(\frac{Q^2}{A}\right)_{j}^{i}\right)+\theta\left(\frac{h_{j+1}^{i+1}-h_{j}^{i+1}}{\Delta x}\right)+$$
$$(1-\theta)\left(\frac{h_{j+1}^{i}-h_{j}^{i}}{\Delta x}\right)+S_f-S_b=0 \quad (5.8)$$

By discretizing the Saint Venant equations they can be used in a simulation to calculate parameters for the open channel model. The mesh shown in figure 5.5 is used to calculate the node (j+1,i+1) by knowing the previous values in time and length (j,i), (j+1,i) and (j,i+1). Therefore some initial condition must be known to calculate the parameters for the open channel in the first iteration. The boundary condition for the flow, at t=0, must be known throughout the pipe. Furthermore, the flow that will enter the channel for $t \leq 0$ must be known, as illustrated with the circles in figure 5.6.

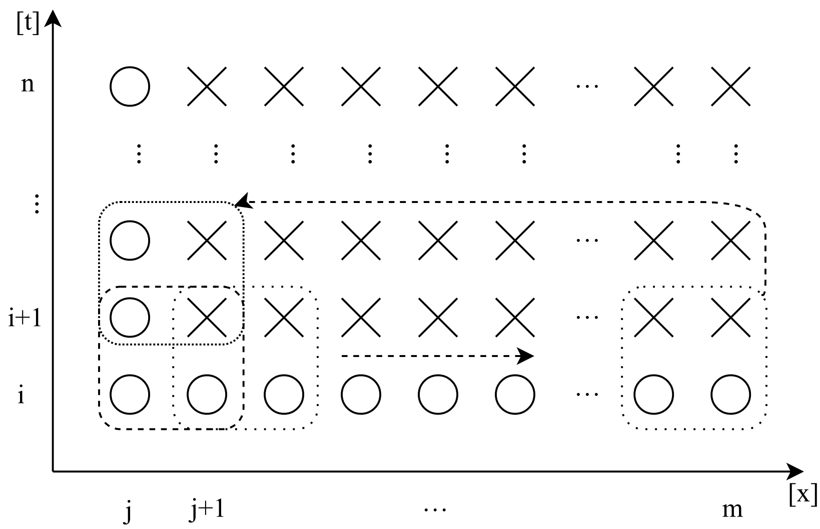

Figure 5.6: Preissmann non-staggered grid scheme example of calculation pattern.

By knowing the flow and parameters for the pipe, the height can be calculated in the initialization nodes, which will be elaborated on later. With equation 5.7, the flow (j+1,i+1) can be calculated by knowing the flow and height in the previous nodes (j,i), (j+1,i) and (j,i+1) as illustrated with the box in the left bottom corner in figure 5.6.

For the Preissmann scheme to be numerical stable the θ parameter is $\theta \leq 0,5$. Does closer θ is to 0,5 the more accurate it is, however it is also more likely to be unstable, therefore from [Krvavica and Travaš, 2014] it is suggested to place θ in the range of $0,55 \leq \theta \leq 0.65$ for practical analysis.

In the following section, the calculating of the flow and height in each node will be explained.

Iteration scheme

[1] In this section, it will be elaborated how the calculation of the flow and height in each iteration is done [Michelsen, 1976].

The discretized continuity equation 5.7 from section 5.2, stated below, is solved for the desired flow in equation 5.10,

$$\theta\frac{Q_{j+1}^{i+1}-Q_j^{i+1}}{\Delta x}+(1-\theta)\frac{Q_{j+1}^{i}-Q_j^{i}}{\Delta x}+\frac{1}{2}\frac{A_{j+1}^{i+1}-A_{j+1}^{i}}{\Delta t}+\frac{1}{2}\frac{A_{j}^{i+1}-A_{j}^{i}}{\Delta t}=0 \tag{5.9}$$

$$Q_{j+1}^{i+1}=-\frac{1}{2\theta}\cdot\left(A_{j+1}^{i+1}-H\right)\cdot\frac{\Delta x}{\Delta t} \tag{5.10}$$

Where H is a parameter for the previous flows and areas in time and section which are known as these are either been set to a specific input at time 0 to t and throughout the pipe, for t=0 as shown in figure 5.6 or has been calculated as the scheme have been iterated.

$$H=\left(2\cdot(1-\theta)\cdot Q_j^i-2\cdot(1-\theta)\cdot Q_{j+1}^i+2\theta Q_j^{i+1}\right)\cdot\frac{\Delta t}{\Delta x}-A_j^{i+1}+A_j^i+A_{j+1}^i \tag{5.11}$$

Instead of using the the second saint venant equation as explained in ??? [2] an equation for calculating the flow in a circular pipe will be used:

$$Q=\left(0.46-0.5\cdot cos\left(\pi\frac{h}{d}\right)+0.04\cdot cos\left(2\pi\frac{h}{d}\right)\right)\cdot Q_f \tag{5.12}$$

This equation describes the flow in a circular pipe by knowing the diameter, d height, h and the flow for a filled pipe Q_f. Where Q_f is calculated as:

$$Q_f=-72\cdot\left(\frac{d}{4}\right)^{0.635}\pi\cdot\left(\frac{d}{2}\right)^2\cdot I_e^{0,5} \tag{5.13}$$

Q_f is calculated from Mannings eqaution and can be seen in appendix A.4. Where I_e is a friction term. [3] [4]

In equation 5.10 the flow Q_{j+1}^{i+1} is a function of the unknown area A_{j+1}^{i+1}, and by subtracting the flow on each side the following is achieved,

$$0=-Q_{j+1}^{i+1}-\frac{1}{2\theta}\cdot\left(A_{j+1}^{i+1}-H\right)\cdot\frac{\Delta x}{\Delta t} \tag{5.14}$$

By calling the right hand side of equation 5.14 for V the following is obtained,

$$V=-Q_{j+1}^{i+1}-\frac{1}{2\theta}\cdot\left(A_{j+1}^{i+1}-H\right)\cdot\frac{\Delta x}{\Delta t} \tag{5.15}$$

[1] FiXme Note: This subsec needs to get canned
[2] FiXme Note: ref tilbage til hvor vi vaelger den fra
[3] FiXme Note: skal der skrives her, at det er antaget at friction er lig med haeldning?
[4] FiXme Note: lav hjaelpe formeller

Equation 5.15 can now be solved by finding the zero for the function V using newton method. However there are still two unknowns in equation 5.15, Q_{j+1}^{i+1} and A_{j+1}^{i+1}. Q_{j+1}^{i+1} can be replaced with equation 5.12 for calculating the flow.

Equation 5.12 is inserted into equation 5.15 and thereby the following is obtained,

$$V = -Q_f \cdot \left(0,46 - 0,5 \cdot cos\left(\pi \frac{h_{j+1}^{i+1}}{d}\right) + 0,04 \cdot cos\left(2\pi \frac{h_{j+1}^{i+1}}{d}\right)\right) \frac{\Delta t}{\Delta x} - \frac{1}{2\theta}\left(A_{j+1}^{i+1} - H\right) \tag{5.16}$$

Furthermore Q_f from equation 5.13 is inserted into equation 5.16,

$$V = -72\left(\frac{d}{4}\right)^{0.635} \pi \cdot \left(\frac{d}{2}\right)^2 I_e^{0,5} \cdot \left(0,46 - 0,5 \cdot cos\left(\pi \frac{h_{j+1}^{i+1}}{d}\right) + 0,04 \cdot cos\left(2\pi \frac{h_{j+1}^{i+1}}{d}\right)\right) \frac{\Delta t}{\Delta x} - \frac{1}{2\theta}\left(A_{j+1}^{i+1} - H\right) \tag{5.17}$$

V is now a function of the height h_{j+1}^{i+1} as the height is the only unknown in finding the area A_{j+1}^{i+1} and the flow for the channel. The area for a circular channel is calculated with the following,

$$A = \frac{d^2}{4} \cdot acos\left(\frac{\frac{d}{2} - h}{\frac{d}{2}}\right) - \sqrt{h \cdot (d-h)} \cdot \left(\frac{d}{2} - h\right) \tag{5.18}$$

As mention the continuity equation 5.17 can be solved by finding the zero for the function V. Newtons method is used to find approximations to the roots/zeros of a real-valued function. By using the Newton method the roots of equation 5.17 can be found, which will correspond to the height of the channel. The approximation is,

$$(h_{j+1}^{i+1})_{k+1} = (h_{j+1}^{i+1})_k - \frac{V_k}{V_k'} \tag{5.19}$$

Where k is the number of iterations, V′ is the differentiated of V with respect to height, $(h_{j+1}^{i+1})_k$ is an initial guess of the root and $(h_{j+1}^{i+1})_{k+1}$ is a better approximation of the height. This calculation is iterated until a satisfied approximation is achieved which fulfills the requirement,

$$\left(h_{j+1}^{i+1}\right)_k - (h_{j+1}^{i+1})_{k-1} < (\epsilon \cdot h_{j+1}^{i+1})_k \tag{5.20}$$

Where ϵ is a small tolerance number, e.g. 5-centimeter variation in water height. Thereby the water height can be found and the area of the water can be calculated with equation 5.18 [5] and thereafter equation 5.10 can be used to calculate the flow of the node.

[5] FiXme Note: afsnit om de forskellige ligninger til beregning af Areal, Ie,Ib,Qf,Q

This calculation is performed for each node in the Preissmann scheme, therefore it is an iterative method of solving the flow for an open channel and in figure 5.7 a flow chart of how these equations are iterated is shown.

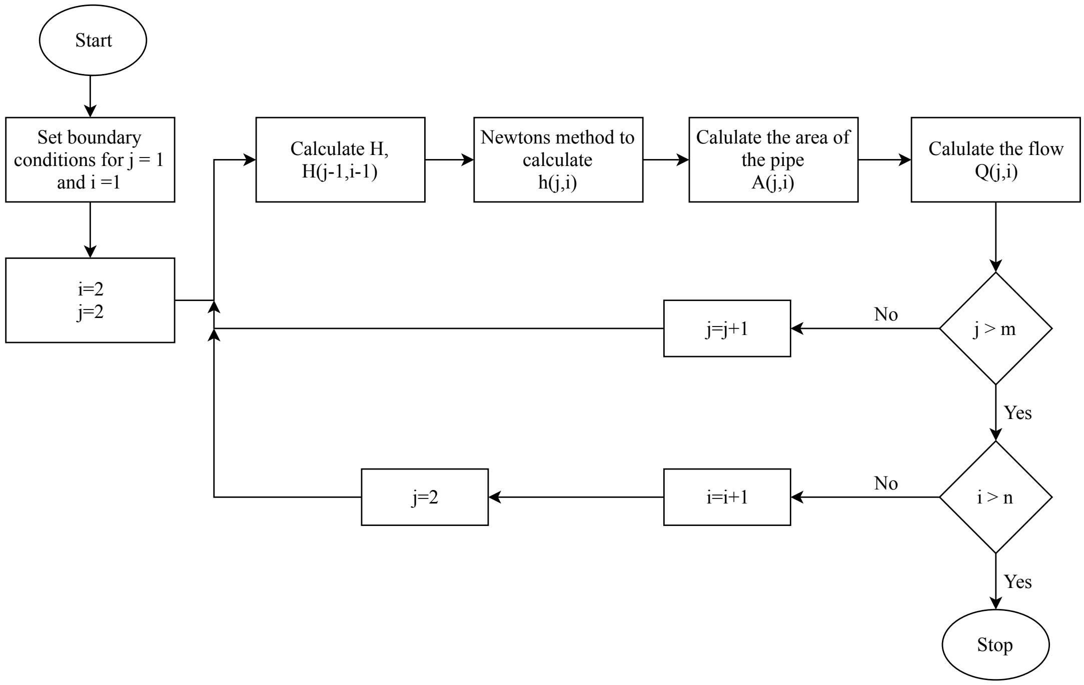

Figure 5.7: Flow chart of the iteration process to calculate the flow in each point.

The iteration scheme starts with setting the boundary conditions for the flow and height as seen in figure 5.6, thereafter i and j are countered one up before starting the iteration process. Hereafter the calculation for H, h, A and Q are conducted in iteratively throughout the channel. Finally, a check is made to investigate if the iteration scheme has been through the whole channel before it steps one up in time. This iteration process will go on until the i $>$ m, which means that all the inputs to the channel has been calculated throughout the pipe.

In the following figures the flow 5.8a and the water height 5.8b for the output of the channel is shown.

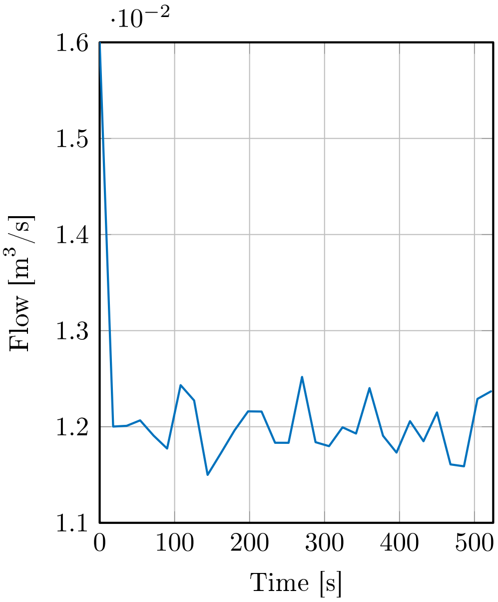

(a)

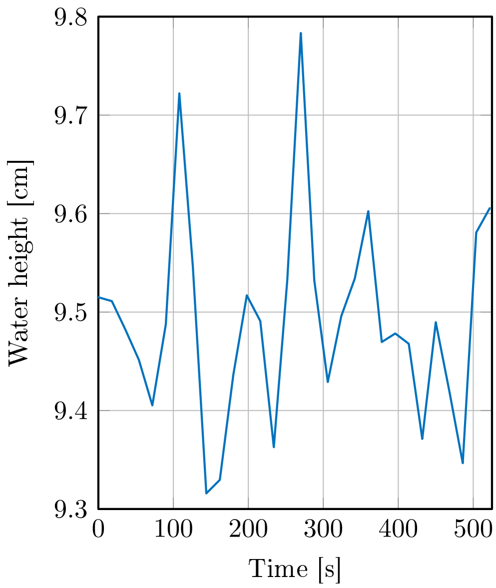

(b)

Figure 5.8: (a) Output flow, (b) the water height at the output of the channel.

[6] These figures shows that whether the height is increasing or decreasing the flow is following, which is what is expected, because a higher water level will result in a higher flow rate and vice versa.

5.3 Concentrate

Various explicit and implicit schemes exists to solve the transport equation obtained in section 4.4 and shown below.

$$A \cdot \frac{\partial C}{\partial t} + Q \cdot \frac{\partial C}{\partial x} = 0 \tag{5.21}$$

As area and flow is already found by solving the Saint-Venant equations by the Preissmann scheme in section 5.2 a simple discretization of the transport equation suffices. The discretized transport equation is shown below:

$$A(x,t) \cdot \frac{C(x,t) - C(x,t-\Delta t)}{\Delta t} + Q(x,t) \cdot \frac{C(x,t) - C(x-\Delta x,t)}{\Delta x} = 0 \tag{5.22}$$

[6] FiXme Note: Paa den her test skal der skrives hvad der testes paa, diameter, hoejde, healdning osv.

Isolating for C(x,t) in steps is shown in the following:

$$\begin{aligned}
&A(x,t) \cdot \tfrac{C(x,t)}{\Delta t} + Q(x,t) \cdot \tfrac{C(x,t)}{\Delta x} = A(x,t) \cdot \tfrac{C(x,t-\Delta t)}{\Delta t} + Q(x,t) \cdot \tfrac{C(x-\Delta x,t)}{\Delta x} \\
&\Updownarrow \\
&C(x,t) \cdot \left(\tfrac{A(x,t)}{\Delta t} + \tfrac{Q(x,t)}{\Delta x}\right) = A(x,t) \cdot \tfrac{C(x,t-\Delta t)}{\Delta t} + Q(x,t) \cdot \tfrac{C(x-\Delta x,t)}{\Delta x} \\
&\Updownarrow \\
&C(x,t) = \tfrac{A(x,t) \cdot \frac{C(x,t-\Delta t)}{\Delta t}}{\frac{A(x,t)}{\Delta t} + \frac{Q(x,t)}{\Delta x}} + \tfrac{Q(x,t) \cdot \frac{C(x-\Delta x,t)}{\Delta x}}{\frac{A(x,t)}{\Delta t} + \frac{Q(x,t)}{\Delta x}} \\
&\Updownarrow \\
&C(x,t) = \tfrac{A(x,t) \cdot C(x,t-\Delta t)}{A(x,t) + Q(x,t) \cdot \frac{\Delta t}{\Delta x}} + \tfrac{Q(x,t) \cdot C(x-\Delta x,t)}{Q(x,t) + A(x,t) \cdot \frac{\Delta x}{\Delta t}}
\end{aligned} \tag{5.23}$$

It can be seen that the concentration can be obtained at current time and place by known values and the solutions of the Saint-Venant equations.

5.4 Implementation & Verification

In this section the suggested structure in section 5.1, implemented with the numerical solutions in section 5.2-5.3, is tested and verified.

The first part to be elaborated upon is the initialization.

Initialization

For the setup procedure of the simulation in list form, the specifications part shown in figure 5.2 needs to be defined. The parameters in the list for both pipe and tank can be seen in table 5.4.

1. Pipe
   - Length [m]
   - Sections (Number of sections the pipe should be split in to)
   - I_b (Slope) [‰]
   - Δx = Length/Sections [m]
   - Diameter [meter]
   - Theta (parameter used in Preissmann scheme)
   - Q_f (maximum flow found by Manning formula, see equation 5.13) [m^3/s]
   - Side/lateral inflow present
   - Section location in data
2. Tank
   - Size [m^3]
   - Height [m]
   - Area = Size / Height [m^2]
   - Maximum outflow [m^3/s]
   - Section location in data

Some parameters can be found from others and is set to be calculated automatically. Furthermore an item is added that indicates in which section of the obtained simulation data the specific output of the component is located. This item is given the number of the order in which the component appears in the list. To give an overview of the system to be simulated, and to easily be able to locate specific parameters needed during simulation, three structures is returned to the workspace. These are named "pipe_spec", "tank_spec" and "sys_setup". The first two structures holds the information shown in table 5.4 respectively. The last one, "sys_setup", holds information of the various parts indexed in the order it should be simulated. In figure 5.9 the content of "sys_setup" is shown for a setup with two pipes an a tank.

Fields	type	component	sections
1	'Pipe'	1	10
2	'Tank'	1	1
3	'Pipe'	1	10
4	'Total'	3	21

Figure 5.9: Display of structure holding system setup information in MATLAB.

Control 6

6.1 Linearization

To be able to obtain a MPC control algorithm the system needs to be transform into state space form. In this section it will be elaborated how this is obtained.

The continuity equation from section ??? and an equation to describe the flow knowing the height is used found in section ????.

$$\frac{\partial A(x,t)}{\partial t} + \frac{\partial Q(x,t)}{\partial x} = 0 \tag{6.1}$$

$$Q = f(h) = \left(0.46 - 0.5 \cdot cos\left(\pi \frac{h}{d}\right) + 0.04 \cdot cos\left(2\pi \frac{h}{d}\right)\right) Q_f \tag{6.2}$$

Equation 6.1 is expanded to the following:

$$\frac{\partial A(h)}{\partial h}\frac{\partial h(x,t)}{\partial t} + \frac{\partial Q(h)}{\partial h}\frac{\partial h(x,t)}{\partial x} = 0 \tag{6.3}$$

By applying the Preissmann scheme from section 5.2 equation 5.5 and 5.6 on the partial derivate of h in terms of time and position, the following is obtained:

$$\begin{aligned} &\frac{\partial A(x,t)}{\partial h}\left(\frac{1}{2}\frac{h_{j+1}^{i+1} - h_{j+1}^{i}}{\Delta t} + \frac{1}{2}\frac{h_{j}^{i+1} - h_{j}^{i}}{\Delta t}\right) + \\ &\frac{\partial Q(x,t)}{\partial h}\left(\theta \frac{h_{j+1}^{i+1} - h_{j}^{i+1}}{\Delta x} + (1-\theta)\frac{h_{j+1}^{i} - h_{j}^{i}}{\Delta x}\right) = 0 \end{aligned} \tag{6.4}$$

This equation can be written on a matrix form:

$$\begin{aligned} &\left[\underbrace{\frac{1}{2\Delta t}\frac{\partial A}{\partial h} - \frac{\theta}{\Delta x}\frac{\partial Q}{\partial h}}_{a} \quad \underbrace{\frac{1}{2\Delta t}\frac{\partial A}{\partial h} + \frac{\theta}{\Delta x}\frac{\partial Q}{\partial h}}_{b}\right]\begin{bmatrix} h_{j}^{i+1} \\ h_{j+1}^{i+1} \end{bmatrix} = \\ -&\left[\underbrace{\frac{-1}{2\Delta t}\frac{\partial A}{\partial h} - \frac{(1-\theta)}{\Delta x}\frac{\partial Q}{\partial h}}_{c} \quad \underbrace{\frac{-1}{2\Delta t}\frac{\partial A}{\partial h} + \frac{\theta}{\Delta x}\frac{\partial Q}{\partial h}}_{d}\right]\begin{bmatrix} h_{j}^{i} \\ h_{j+1}^{i} \end{bmatrix} \end{aligned} \tag{6.5}$$

We want the equation on the normal state space form.

$$\dot{x} = Ax + Bu \tag{6.6}$$

Where A is the system matrix, x is the state of the system, B is the input matrix and u is the input.

$$\underbrace{\begin{bmatrix} 1 & 0 & 0 & \cdots & 0 \\ 0 & b_1 & 0 & \cdots & 0 \\ 0 & a_1 & b_2 & \cdots & \vdots \\ \vdots & \vdots & \ddots & \ddots & 0 \\ 0 & 0 & 0 & a_{m-1} & b_m \end{bmatrix}}_{\xi} \underbrace{\begin{bmatrix} h_0^{i+1} \\ h_1^{i+1} \\ h_2^{i+1} \\ \vdots \\ h_m^{i+1} \end{bmatrix}}_{\dot{x}} = \underbrace{\begin{bmatrix} 0 & 0 & 0 & \cdots & 0 \\ c_0 & d_1 & 0 & \cdots & 0 \\ 0 & c_1 & d_2 & \cdots & 0 \\ \vdots & \vdots & \ddots & \ddots & \vdots \\ 0 & 0 & 0 & c_{m-1} & d_m \end{bmatrix}}_{A} \underbrace{\begin{bmatrix} h_0^{i} \\ h_1^{i} \\ h_2^{i} \\ \vdots \\ h_m^{i} \end{bmatrix}}_{x} + \underbrace{\begin{bmatrix} 1 \\ -a_0 \\ 0 \\ \vdots \\ 0 \end{bmatrix}}_{B} h_m^{i+1} + \underbrace{\begin{bmatrix} \frac{dh}{dQ} \\ 0 \\ 0 \\ \vdots \\ 0 \end{bmatrix}}_{B_d} Qd_{m+1} \tag{6.7}$$

Where m denotes the channel pieces. To obtain a state space for the matrix to the left needs to inversed, thereby obtaining the following equation:

$$\dot{x} = -\xi^{-1}(Ax + Bu) \tag{6.8}$$

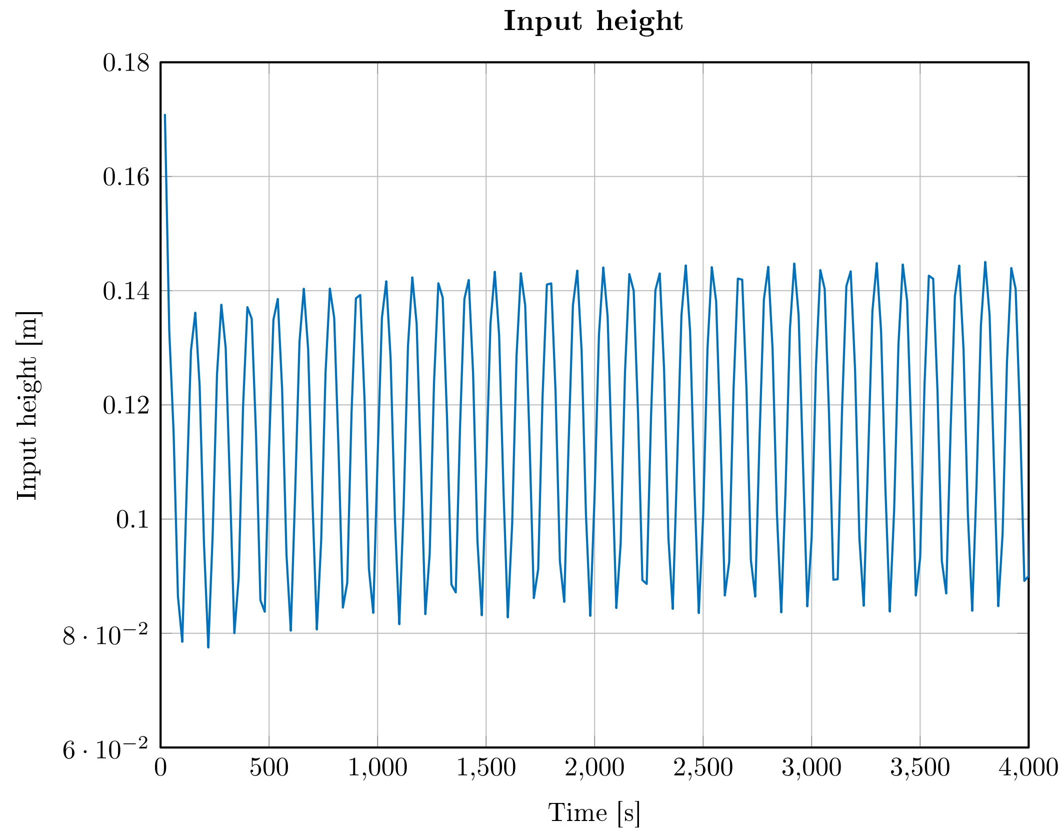

Figure 6.1: Input height for the simulation.

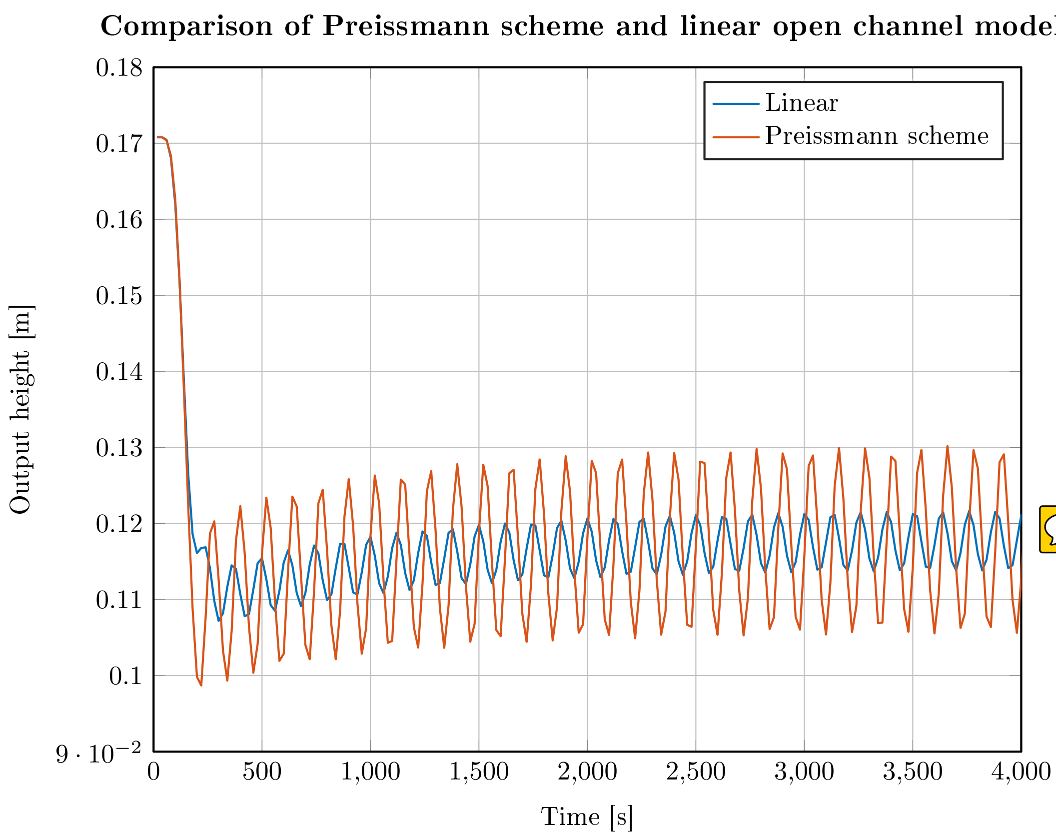

Figure 6.2: Output height for the linear and Preissmann scheme simulation.

6.2 Model predictive control

In this section, the design of the controller is elaborated. First the control problem the design of the Model predictive controller (MPC).

The simulation covered in chapter 5 is to be controlled with respect to the problems elaborated in section 1.4 and stated here.

1. Flow variations due to large industries and natural phenomenons
2. Concentration variations due to large industries and natural phenomenons
   a) Chloride variations
   b) Phosphor variations
   c) Nitrogen variations
   d) Organic matter variations

From the problem statement, it is stated that flow and concentration variations must be kept to a minimum without causing any overflow in the sewer. To achieve this, tanks are used, these are placed in the sewer network to find locations where they are able to hold back disturbance that will otherwise cause flow and concentration variations into the WWTP. However, the output of these tanks must be controlled in a way where overflow in the tank is prohibited. Therefore the controller must control the output of these tanks in an optimal manner to keep the input variations to the WWTP at a minimum and still be controlled according to some constraints.

To obtain such an optimal behavior MPC is chosen as stated in section 1.4. MPC solves a optimizations problem at each time instant, k, where the main point is to compute a control vector, u that is feed to the system.

An MPC algorithm consists of:
Cost function or control objective,$\mathcal{J}$, is an algorithm measuring e.g. the difference between future outputs and a reference while at the same time instant recognizing that any control action is costly for the system. Therefore the price is measured in the cost function over the prediction horizon, H_p. This function is therefore minimized with the respect to the future control vector to keep the cost minimized. Furthermore, only the first control input from the vector is used in each time instant thus this optimization is process is calculated at each time step where a new control input is calculated [Ruscio, 2001].

Constraints is unique advantages of MPC. Constraints can be applied to the process variables e.g. constraints can be set on the states of the system not allowing them to go below a certain value or above. Constraints are usually written as inequality constraint $Ax \leq b$ where the constraint a subject to the optimization problem [Ruscio, 2001].

Prediction model for the MPC to be able to predict future system behavior it needs a model to predict from. The model describes the input output behavior of the system. The model will mainly be used to predict the output of the system over the prediction horizon [Ruscio, 2001].

For MPC to optimize the system a cost function must be written to penalize variations of the flow output $Q(k+i|k)$ and the concentration output $C(k+i|k)$. Where k defines the time step and i value going from $1 \leq H_p$. The cost function for flow and concentration is:

$$\mathcal{J} = \sum_{i=1}^{H_p-1} ||Q(k+i|k)C(k+i|k) - Q(k+i-1|k)C(k+i-1|k)||^2_{\mathcal{Q}(i)} \tag{6.9}$$

Where $\mathcal{J}$ is the cost function that needs to be minimized, Q is the flow, C is the concentration and $\mathcal{Q}$ is a weighting parameter. It has been desired to only look at flow variation in the simulation and thereby excluding concentration from the cost function. This has been done to limit the control problem and ease the computation, to begin with. Thereby the cost function has been rewritten to:

$$\mathcal{J} = \sum_{i=1}^{H_p-1} ||\hat{y}(k+i|k) - \hat{y}(k+i-1|k)||^2_{\mathcal{Q}(i)} \tag{6.10}$$

$$\begin{aligned} \text{s.t.} \quad \hat{x}(k+i+1) &= A\hat{x}(k+i|k) + B\hat{u}(k+i|k) + B_d d(k+i|k) \\ \hat{y}(k+i) &= C\hat{x}(k+i|k) \\ \underline{x} \leq \hat{x} &\leq \overline{x} \end{aligned} \tag{6.11}$$

Where Q has been replaced with the output y as it can be measured directly from the state space system. The hat denotes a small signal value and not an estimate for y. y corresponds to the height of the wastewater in the channel, however, it is the same to minimize height difference as the flow because both describe the variation in the output of the sewer. Furthermore, the cost function is subject to constraints for the states. The states have a lower and upper constraint corresponding respectively to the bottom of the channel and the top of the channel, denoted respectively with $\underline{x}$ and $\overline{x}$. In order for the controller to minimize the variations in the output, it must be able to predict future events from knowing the current state. Therefore, by iterating the linear model up to the prediction horizon the controller is able to predict future states [Maciejowski, 2002]. Thus by using the state equation recursively the state equation can be predicted up to the prediction horizon as shown in equation 6.12:

$$\begin{aligned} \hat{x}(k+1|k) &= A\hat{x}(k|k) + B\hat{u}(k|k) + B_d d(k|k) \\ \hat{x}(k+2|k) &= A\hat{x}(k+1|k) + B\hat{u}(k+1|k) + B_d d(k+1|k) \\ &= A^2\hat{x}(k|k) + AB\hat{u}(k|k) + AB_d d(k|k) + B\hat{u}(k+1|k) \\ &+ B_d d(k+1|k) \\ &\vdots \\ \hat{x}(k+H_p|k) &= A\hat{x}(k+H_p-1|k) + B\hat{u}(k+H_p-1|k) + B_d d(k+H_p-1|k) \\ &= A^{H_p}\hat{x}(k|k) + A^{H_p-1}B\hat{u}(k|k) + A^{H_p-1}B_d d(k|k) + \cdots + \\ &+ B\hat{u}(k+H_p-1|k) + B_d d(k+H_p-1|k) \end{aligned} \tag{6.12}$$

Here the first equation $\hat{x}(k+1|k)$ is inserted into the second and this is iterated up to the prediction horizon. This can be setup as prediction vectors and matrices denoted by

$\mathcal{X}, \mathcal{A}, \mathcal{B}, \mathcal{U}, \mathcal{B}_d$ and $\mathcal{D}$:

$$
\begin{aligned}
\underbrace{\begin{bmatrix} \hat{x}(k+1|k) \\ \hat{x}(k+2|k) \\ \vdots \\ \hat{x}(k+H_p|k) \end{bmatrix}}_{\mathcal{X}} &= \underbrace{\begin{bmatrix} A \\ A^2 \\ \vdots \\ A^{H_p} \end{bmatrix}}_{\mathcal{A}} \hat{x}(k|k) \\
&+ \underbrace{\begin{bmatrix} B & 0 & \cdots & 0 \\ AB & B & \cdots & 0 \\ \vdots & \vdots & \ddots & \vdots \\ A^{H_p-1}B & A^{H_p-2}B & \cdots & B \end{bmatrix}}_{\mathcal{B}} \underbrace{\begin{bmatrix} \hat{u}(k|k) \\ \hat{u}(k+1|k) \\ \vdots \\ \hat{u}(k+H_p-1|k) \end{bmatrix}}_{\mathcal{U}} \\
&+ \underbrace{\begin{bmatrix} B_d & 0 & \cdots & 0 \\ AB_d & B_d & \cdots & 0 \\ \vdots & \vdots & \ddots & \vdots \\ A^{H_p-1}B_d & A^{H_p-2}B_d & \cdots & B_d \end{bmatrix}}_{\mathcal{B}_d} \underbrace{\begin{bmatrix} d(k|k) \\ d(k+1|k) \\ \vdots \\ d(k+H_p-1|k) \end{bmatrix}}_{\mathcal{D}}
\end{aligned}
\tag{6.13}
$$

Where $\mathcal{X}$ is the predicted state vector for the entire prediction horizon. $\mathcal{A}$ is the state matrix up to the prediction horizon. $x(k|k)$ is the initial state and is used to predict the hole prediction horizon, $\mathcal{B}$ is the input matrix for the prediction horizon, $\mathcal{U}$ is the predicted input vector, which consists of all the predicted inputs from the current timestep until $(k + H_p - 1)$. $\mathcal{B}_d$ is the disturbance matrix for the prediction horizon and $\mathcal{D}$ is the disturbance vector.

This iteration process is also done for the output equation:

$$
\mathcal{Y}(k) = \begin{bmatrix} y(k+1|k) \\ y(k+2|k) \\ \vdots \\ y(k+H_p-1|k) \end{bmatrix} = \underbrace{\begin{bmatrix} C & 0 & \cdots & 0 \\ 0 & C & \cdots & 0 \\ \vdots & \vdots & \ddots & 0 \\ 0 & 0 & 0 & C \end{bmatrix}}_{\mathcal{C}} \begin{bmatrix} \hat{x}(k+1|k) \\ \hat{x}(k+2|k) \\ \vdots \\ \hat{x}(k+H_p|k) \end{bmatrix}
\tag{6.14}
$$

Where $\mathcal{C}$ is a diagonal matrix with the output matrix C and $\mathcal{X}$ the predicted state vector. By inserting the predicted state equation 6.13, into the predicted output equation 6.14 the following is achieved:

$$
\mathcal{Y}(k) = \mathcal{C}\mathcal{A}x(k) + \mathcal{C}\mathcal{B}\mathcal{U}(k) + \mathcal{C}\mathcal{B}_d\mathcal{D}(k)
\tag{6.15}
$$

By using the following notation on equation 6.15:

$$
\psi = \mathcal{C}\mathcal{A} \qquad \gamma = \mathcal{C}\mathcal{B} \qquad \Theta = \mathcal{C}\mathcal{B}_d
\tag{6.16}
$$

The predicted output equation can be rewritten as:

$$\mathcal{Y}(k) = \psi x(k) + \gamma\mathcal{U}(k) + \Theta\mathcal{D}(k) \tag{6.17}$$

To be able to use the cost function, equation 6.10, it has to be rewritten so the predicted output equation can be used. This is done by replacing the output y with the predicted output $\mathcal{Y}$ thereby the following is obtained:

$$\mathcal{J} = ||\mathcal{Y}(k) - \mathcal{Y}(k-1)||^2_{\mathcal{Q}(i)} \tag{6.18}$$

Where the difference between $\mathcal{Y}(k)$ and $\mathcal{Y}(k-1)$ can be expressed as:

$$\Delta\mathcal{Y}(k) = \mathcal{Y}(k) - \mathcal{Y}(k-1) \tag{6.19}$$

Thereby the following cost function is achieved:

$$J = \Delta\mathcal{Y}(k)^T \cdot Q \cdot \Delta\mathcal{Y}(k) \tag{6.20}$$

To be able to write the cost function as quadratic and linear terms of the predicted output $\Delta\mathcal{U}$, equation 6.17 is therefore inserted into equation 6.20 and thereby the following is obtained:

$$\mathcal{J} = (\psi\Delta x(k) + \gamma\Delta\mathcal{U}(k) + \Theta\Delta\mathcal{D}(k))^T \cdot Q \cdot (\psi\Delta x(k) + \gamma\Delta\mathcal{U}(k) + \Theta\Delta\mathcal{D}(k)) \tag{6.21}$$

The term on the right hand side of equation 6.21 is equal to:

$$\begin{aligned}
&(\psi\Delta x(k) + \gamma\Delta\mathcal{U}(k) + \Theta\Delta\mathcal{D}(k))^T \cdot Q \cdot (\psi\Delta x(k) + \gamma\Delta\mathcal{U}(k) + \Theta\Delta\mathcal{D}(k)) = \\
&\Delta x(k)^T\psi^T Q\psi\Delta x(k) + \underbrace{\Delta x(k)^T\psi^T Q\gamma\Delta\mathcal{U}(k)}_{Linear} + \Delta x(k)^T\psi^T Q\Theta\Delta\mathcal{D}(k) \\
&\underbrace{\Delta\mathcal{U}(k)^T\gamma^T Q\psi\Delta x(k)}_{Linear} + \underbrace{\Delta\mathcal{U}(k)^T\gamma^T Q\gamma\Delta\mathcal{U}(k)}_{Quadratic} + \underbrace{\Delta\mathcal{U}(k)^T\gamma^T Q\Theta\Delta\mathcal{D}(k)}_{Linear} \\
&\Delta\mathcal{D}(k)^T\Theta^T Q\psi\Delta x(k) + \underbrace{\Delta\mathcal{D}(k)^T\Theta^T Q\gamma\Delta\mathcal{U}(k)}_{Linear} + \Delta\mathcal{D}(k)^T\Theta^T Q\Theta\Delta\mathcal{D}(k)
\end{aligned} \tag{6.22}$$

Here the quadratic and linear terms of $\Delta\mathcal{U}$ are denoted respectively, the remaining terms are the constants and these are not denoted in the equation, however, they will be referred to in the following equations as, c. The quadratic variables are collected in:

$$\mathcal{H} = \gamma^T Q\gamma \tag{6.23}$$

And the linear variables are collected in:

$$\mathcal{G} = 2\Delta x(k)^T \psi^T Q\gamma + 2\Delta\mathcal{D}(k)^T \Theta^T Q\gamma \tag{6.24}$$

Thereby inserting these expressions in equation 6.22 the final cost function is obtained:

$$\min_{\Delta\mathcal{U}(k)} \mathcal{J}(\Delta\mathcal{U}(k)) = \min_{\Delta\mathcal{U}(k)} \Delta\mathcal{U}(k)^T \mathcal{H}\Delta\mathcal{U}(k) + \mathcal{G}\Delta\mathcal{U}(k) + c \tag{6.25}$$

Constraints

In order to apply the constraints, shown in equation 6.10 for the states, to the optimization problem in equation 6.25 the constraints must be reformulated so they are a constraint of the controller input $\Delta\mathcal{U}$, therefore it is required to reformulate the inequalities constraints.

The constraints applied to the states are upper and lower bound to the channel and the tank, thereby not allowing the simulation to overfill the channel or the tank, or, to have a negative height in either of the two. In the following equation the constraint for the states is shown:

$$\underline{x} \le \hat{x} \le \overline{x} \tag{6.26}$$

As the $\hat{x}$ is a small signal value and as the constraint is for full signal values the operating point needs to be subtracted from the lower and upper bounds thereby transforming the lower and upper bound to small signals:

$$\underline{x} - \bar{x} \le \hat{x} \le \overline{x} - \bar{x} \tag{6.27}$$

To reformulated the constraint the predicted state equation 6.13 is inserted instead of the state vector.

$$\underline{x} - \bar{x} \le \mathcal{A}\hat{x} + \mathcal{B}\mathcal{U} + \mathcal{B}\mathcal{D} \le \overline{x} - \bar{x} \tag{6.28}$$

However, to make the constraint depend on $\Delta\mathcal{U}$ the difference between the current timestep and the previous timestep, $\Delta\mathcal{U}(k) = \Delta u(k) - \Delta u(k-1)$, is inserted on the state, input and disturbance:

$$\underline{x} - \bar{x} \le \mathcal{A}(\Delta\hat{x}(k) + x(k-1)) + \mathcal{B}(\Delta\mathcal{U}(k) + \mathcal{U}(k-1)) + \mathcal{B}(\Delta\mathcal{D}(k) + \mathcal{D}(k-1)) \le \overline{x} - \bar{x} \tag{6.29}$$

Now the constraint is set up as a constraint on the input signal. In addition, the constraint has to be setup as equality constraints, therefore, it is divided into two constraints:

$$\underbrace{\underline{x} - \bar{x} - \mathcal{A}(\Delta\hat{x}(k) + x(k-1)) - \mathcal{B}(\Delta\mathcal{D}(k) + \mathcal{D}(k-1)) - \mathcal{B}u(k-1)}_{x_1} \le \mathcal{B}\Delta\mathcal{U} \tag{6.30}$$

$$\underbrace{\overline{x} - \bar{x} - \mathcal{A}(\Delta\hat{x}(k) + x(k-1)) - \mathcal{B}(\Delta\mathcal{D}(k) + \mathcal{D}(k-1)) - \mathcal{B}u(k-1)}_{x_2} \geq \mathcal{B}\Delta\mathcal{U} \tag{6.31}$$

The constraints can be setup on the standard inequality constraint form and thereby be included in the algorithm for the MPC implementation.

$$\begin{bmatrix} \mathcal{B} \\ -\mathcal{B} \end{bmatrix} \Delta\mathcal{U} \leq \begin{bmatrix} x_1 \\ x_2 \end{bmatrix} \tag{6.32}$$

In the following section the implementation of the cost function and constraints, shown in this section, in MATLAB will be elaborated

6.2.1 Implementation of MPC

In this section the implementation of MPC in MATLAB will be elaborated.

The cost function in equation 6.25 is setup as a quadratic. In order to solve this minimization problem and find a global minimum quadratic programming (QP) is used. In MATLAB there well develop solvers for QP problems, in this project the quadprog function has been chosen. Quadprog solves the minimization problem subject to constraints to the specified convex objective function.

Bibliography

[AquaEnviro, 2010] AquaEnviro (2010). Fungal problems in wastewater treatment works. Website. Posted 16th June 2010 - https://www.aquaenviro.co.uk/fungal-problems-in-wastewater-treatment-works/.

[Boysen, 2011] Boysen, H. (2011). k_v: what, why, how, whence? Technical report, Danfoss.

[College, 2018] College, M. E. C. (2018). Biological components of wastewater. Website. http://water.me.vccs.edu/courses/ENV149/biological.htm.

[Eniro, 2018] Eniro (2018). www.krak.dk.

[EPA, 1994] EPA (1994). How wastewater treatment works... the basics. website. https://www3.epa.gov/npdes/pubs/bastre.pdf.

[Eschooltoday, 2017] Eschooltoday (2017). Liquid waste (sewage/wastewater) treatment. Website. http://eschooltoday.com/pollution/water-pollution/sewage-treatment-process-for-kids.html.

[Fredericia-Spildevand, 2018a] Fredericia-Spildevand (2018a). Geographical information systems. A map to describe the length, slope and size of the different sewers in Fredericia. http://frsp.webgrafkort.dk/Mainpage.aspx.

[Fredericia-Spildevand, 2018b] Fredericia-Spildevand (2018b). Summary of company visits. Summary from a meeting with Fredericia Spildevand og Energi A/S can be found in appendix A.1.

[Hvitved-Jacobsen et al., 2013] Hvitved-Jacobsen, T., Vollertsen, J., and Nielsen, A. H. (2013). *Sewer processes: microbial and chemical process engineering of sewer networks*. CRC press.

[Institue of hydromechanics,] Institue of hydromechanics. Concepts, definitions and the diffusion equation. Technical report, Karlsruhe Institute of Technology.

[Kallesøe, 2005] Kallesøe, C. S. (2005). Fault detection and isolation in centrifugal pumps. ISBN-10: 87-90664-22-1.

[Krvavica and Travaš, 2014] Krvavica, N. and Travaš, V. (2014). A comparison of method of characteristics and preissmann scheme for fllod propagation modeling with 1d saint-venant equations. *Open Access Journal*.

[Maciejowski, 2002] Maciejowski, J. M. (2002). *Predictive control: with constraints*. Pearson education.

[Mays, 2001] Mays, L. W. (2001). *Stormwater collection systems design handbook*. McGraw-Hill Professional.

[Michelsen, 1976] Michelsen, H. (1976). Ikke-stationær strømning i delvis fyldte kloakledninger. Master's thesis, Den kongelige veterinær og landbohøjskole.

[Munson et al., 1998] Munson, B. R., Young, D. F., and Okiishi, T. H. (1998). *Fundamentals of fluid mechanics*. Wiley.

[Nykredit, 2018] Nykredit (2018). Familietyperne. website. website - https://www.mitnykredit.dk/privat/info/bank/forbrugsoverblik-familietyper.xml.

[Prabhata K. Swamee, 2008] Prabhata K. Swamee, A. K. S. (2008). Design of water supply pipe networks. ISBN-13:9780470225042, Publisher: John Wiley and Sons.

[Rinkesh, 2009] Rinkesh (2009). What is wastewater treatment. website. https://www.conserve-energy-future.com/process-of-wastewater-treatment.php.

[Rossi et al., 2014] Rossi, F., Motta, O., Matrella, S., Proto, A., and Vigliotta, G. (2014). Nitrate removal from wastewater through biological denitrification with oga 24 in a batch reactor. *Water*, 7(1):51–62.

[Ruscio, 2001] Ruscio, D. D. (2001). Model predictive control and optimization. Lecture notes. Lecture notes on Model Predictive Control.

[Schlütter, 1999] Schlütter, F. (1999). *Numerical modelling of sediment transport in combined sewer systems*. PhD thesis, The Hydraulics and Coastal Engineering Group, Dept. of Civil Engineering, Aalborg University.

[Schütze et al., 2011] Schütze, M., Butler, D., and Beck, B. M. (2011). *Modelling, simulation and control of urban wastewater systems*. Springer Science & Business Media.

[Sjøholm, 2016] Sjøholm, P. (2016). Rensningsanlæg (wastewater plant). Video. $https://www.youtube.com/watch?v = cEQ\_INO6OlE$.

[Statistics-Denmark, 2018] Statistics-Denmark (2018). Population according to cities in 2017. https://www.dst.dk/en.

[Szymkiewiczi, 1998] Szymkiewiczi, R. (1998). *Numerical Modeling in Open Channel Hydraulics*. Springer.

[Vestergaard, 1989] Vestergaard, K. (1989). *Numerical Modelling of Streams: Hydrodynamic models and models for transport and spreading of pollutants*. PhD thesis, Hydraulic & Coastal Engineering Laboratory, Department of Civil Engineering, Aalborg University.

[Vojtesek et al.,] Vojtesek, J., Dostal, P., and Maslan, M. Modelling and simulation of water tank.

Appendix A

A.1 Summary of company visits

This appendix contains a summary from a meeting with the Fredericia wastewater department. The summary is in danish.

Virksomheds besøg 19/03/2018

Spildevand der kommer til rensning ved Fredericia rensninganlæg stammer hovedsageligt fra industrien, 60-65 %. Ved Carlsberg og Arla er der flow målinger. Der er ikke målinger fra beboelse, hverken flow eller koncentrat, dog er der flow målinger ved nogle af pumpe stationer, samt flow og koncentrations målinger ind på rensningsanlægget. Stofmængden er ukendt fra det meste af industrien. Der er biotector ved Carlsberg (TOC) og COD måler ved Arla. Fredericia kunne evt. skaffe flowmålinger til os efter kontakt med industrien. På nuværende tidspunkt regulerer Carlsberg deres spildevand så det har en pH værdi mellem 6 og 9. Carlsberg har også et spare bassin. Arla har to spare bassiner, hvor de også kontrollere deres pH udledning. Shell har deres eget rensningsanlæg. Industrien er typisk gode til at holde en konsistent udledning af flow og koncentrat, der kan dog forekomme uheld. Fordelene ved Fredericia er, at temperaturen på spildevandet i kloakkerne ligger omkring 16-17 grader året rundt. Dette hjælper bakterierne med denitrificering af spildevandet. Bakterierne er mindre aktive med nitrificeringen og denitrificering når temperaturen kommer under 10 grader celsius. Hvilket betyder, at fjernelsen af nitrogen går langsommere.

- Der er problemer i ledningsnettet når der falder kraftig regn, der kan forekommer overløb, derudover gør man rensningsprocessen hurtigere ved kun at føre vandet igennem den mekaniske rensning og derefter udlede det til Lillebælt.
- Der er kul filter på næsten alt for at fjerne lugtgener, såsom dæksler, overtryksventiler og lukkede bassiner.
- Man vil gerne minimere opholdstid i spare bassiner for at undgå produktion af hydrogen sulfid.
- Ved vedligeholdelse af rensningsanlægget lukkes hovedledningen ind til rensningsanlægget, hvor det er muligt at stuve spildevand op i hoved ledning i 3-4 timer i tørvejr.
- Grundvandsindtrængning er forhøjet under regnvejr, samt forhøjet når vandstanden i Lillebælt er over normen.
  - Forhøjet vandstand kan øge klorid indholdet i spildevandet både ved at trænge ind gennem grundvandet, men også ved tilbageløb i overløbsanlæg beliggende ud til Lillebælt. Dette er et problem, da bakterierne fungerer bedst med en konstant mængde af klorid i spildevandet. Variationer i klorid gør, at bakteriernes nedbrydningsproces af de forskellige stoffer i spildevandet er nedsat for en periode. Når indholdet af klorid er konstant igen tilpasser bakterierne sig og deres nedbrydningsproces går tilbage til normal kapacitet.
- Der er ingen forfældning i rensningsanlægget pga. luftgener.

  - Har tidligere udtaget primær slam ved bundfældning, det blev stoppet pga. høj gas udvikling, da dette gav lugtgener.
  - Der planlægges igen at udtage primær slam ved en filtreringsproces for at undgå lugtgener.
- Fosfor kommer hovedsageligt fra industri ca. 300-500 kg/døgn under normal drift. Fosfor er nødvendigt da dette indgår i processen til at nedbryde kvælstof.
- Varierende indhold af klorid i spildevandet er et problem for bakterierne, dette er især et problem under 10 mg/l.
- Rensningsanlægget har en kapacitet på 420.000 People Equivalent (PE), PE svarer til 120 COD/døgn eller 0,2 mg/l/døgn for en person.
- Når der er tørvejr er der et typisk flow på 800-1200 $m^3/time$ ind til rensningsanlægget.

Det ideelle scenarie er,

- Konstant flow og koncentrat
- Fast indhold af koncentrat (Klorid bl.a.)
  - Nødvendigvis ikke et lavt indhold

Prioriteringer i forhold til forstyrrelse i styring af ledningsnetværk.

- Små klorid variationer
- Slam/bakterier nok til at kunne omsætte kvælstof
  - Dette reguleres der for i rensningsanlægget.
- Der skal være en hvis mængde kulstof
  - Hvis spildevand flowet er konstant, er dette ikke et problem for rensningsanlægget.
- Små flow variationer
- Lav opholdstid i bassiner

A.2 Pump information

Information regarding some of the pumps in Fredericia.

In tabluar A.1 information regarding the pumps located in Fredericia can be found. These values have been given by Fredericia.

Location	Pump capacity $[m^3/s]$	Number of pumps	Surface area of the well $[m^2]$	Start/stop level [m]	Wear reduction [%]	Total pumping capacity $[m^3/s]$
Damvej P215	0,0478	2	12.56	0,7/0,37	5-10	0.0956
Thulesvej P217	0,0719	2	12.56	0,59/0,07	25-30	0.1438
Treldevej P218	0,0206	1	7.06	0,67/0,17	25-30	0,0206
Treldevej east P219	0,0214	2	12.56	0,79/0,34	25-30	0,0428
Lillebælts allé P221	0,0138	2	6	1,06/0,7	5-10	0,0276
Benzinvej P254	0,0476	2	12.56	1/0.36	5-10	0,0952
Norgesgade P255	0,350	3	N/A	N/A	N/A	1,05
Vesthavnsvej P256	0,240	5	N/A	N/A	N/A	1,2

Table A.1: Information for the different pumps located in Fredericia

A.3 Flow profiles

Zone	**Residential area** $[km^2]$	**Industrial area** $[km^2]$	**Population per area**
1,1	0,167	0,0083	517
1,2	0,111	-	344
1,3	0,458	0,543	1418
2	0,056	-	173
3	0,167	-	517
4,1	1,125	0,375	3485
4,2	0,167	-	517
4,3	0,580	-	1797
5	0,104	-	322
6	0,115	-	356
7	0,771	0,014	5874
8 - 9	0,667	0,021	2067
10,1	0,903	0,333	3916
10,2	1,781	-	7832
11	0,278	-	865
Total area	7,45	1,294	30000

Table A.2: Table of the sizes of the residential and industrial areas and the population in the residential areas [Nykredit, 2018].

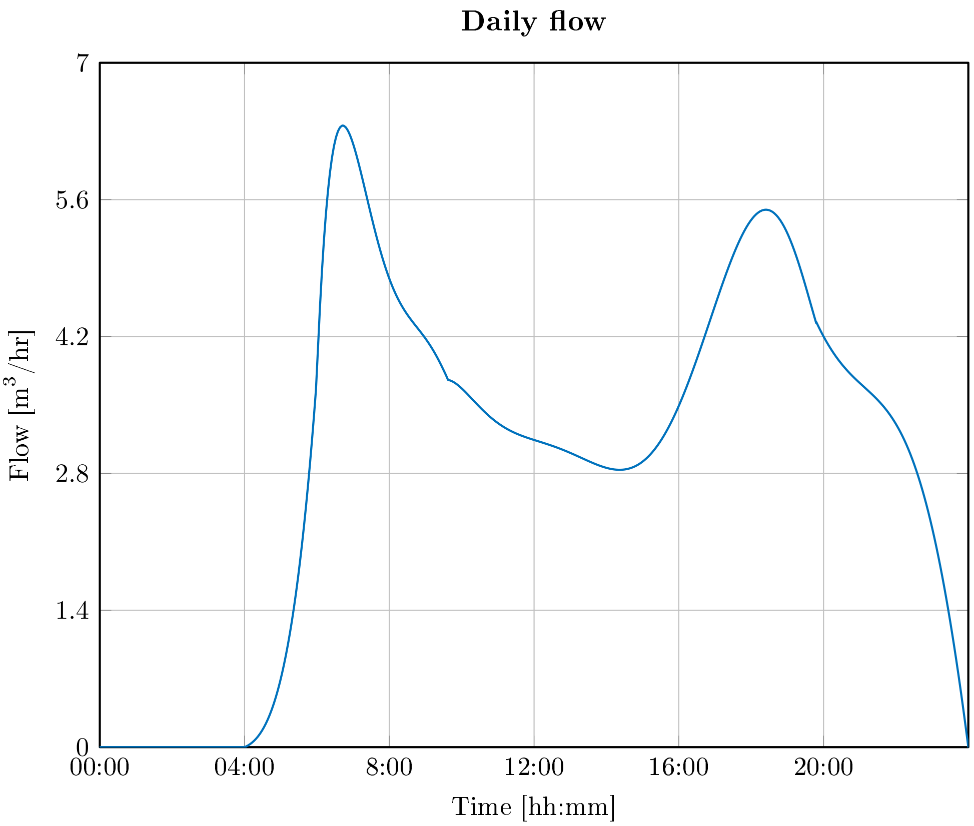

Figure A.1: A flow profile for Thulesvej.

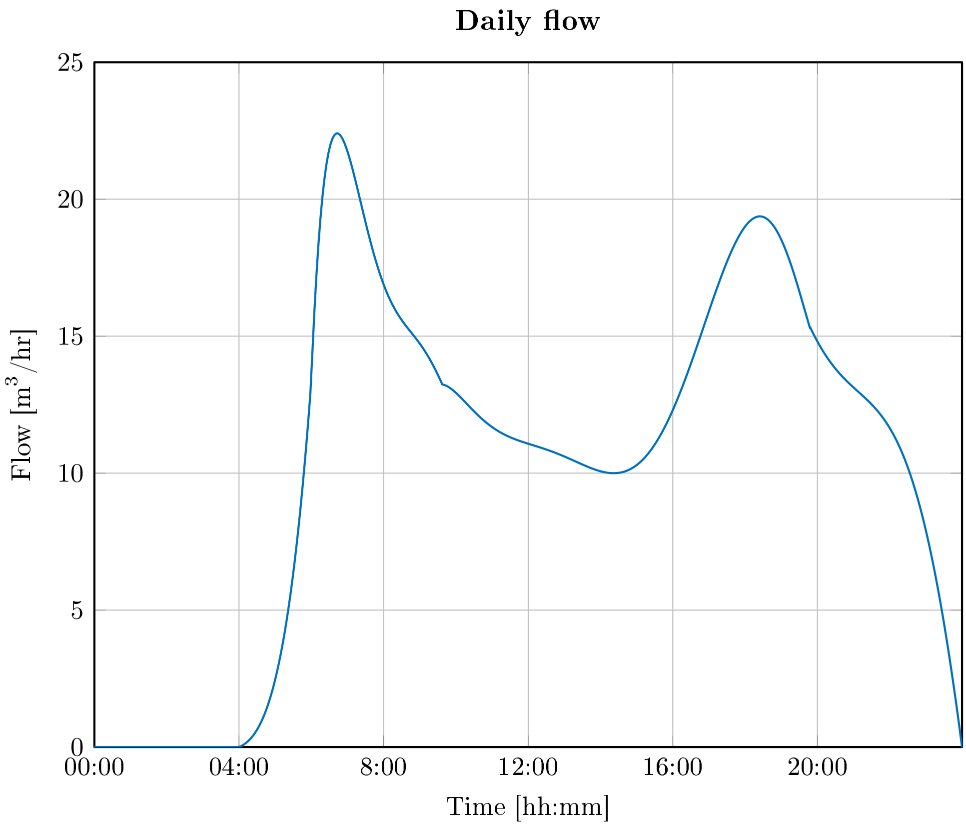

Figure A.2: A flow profile for Thulesvej.

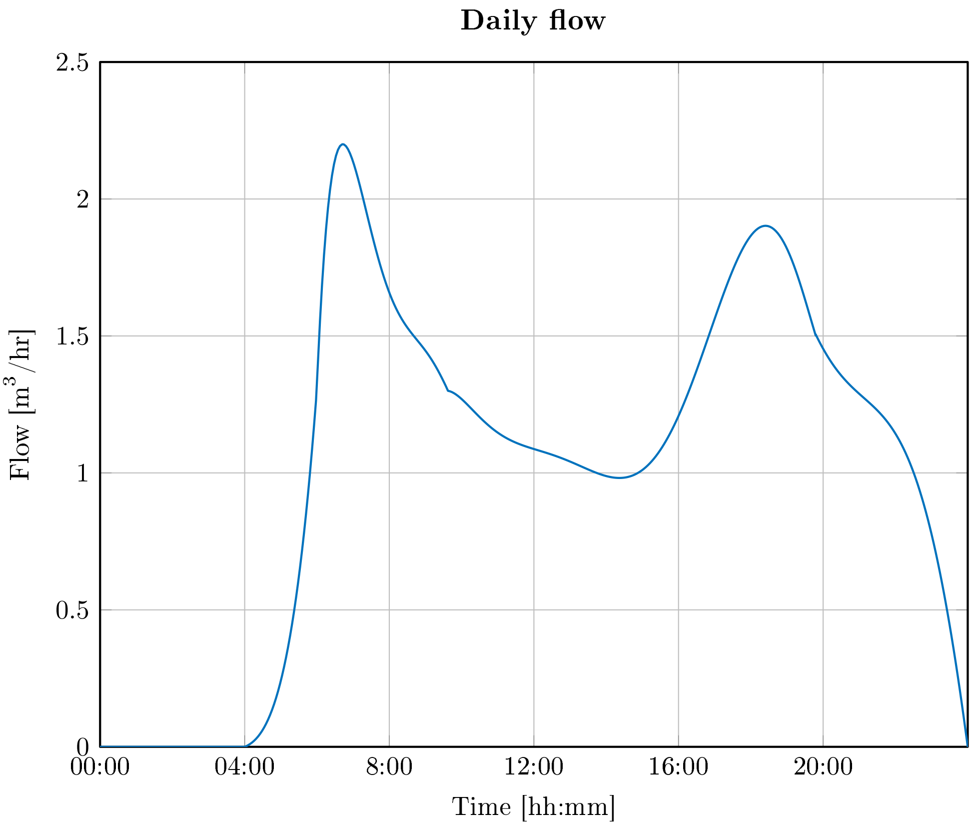

Figure A.3: A flow profile for Thulesvej.

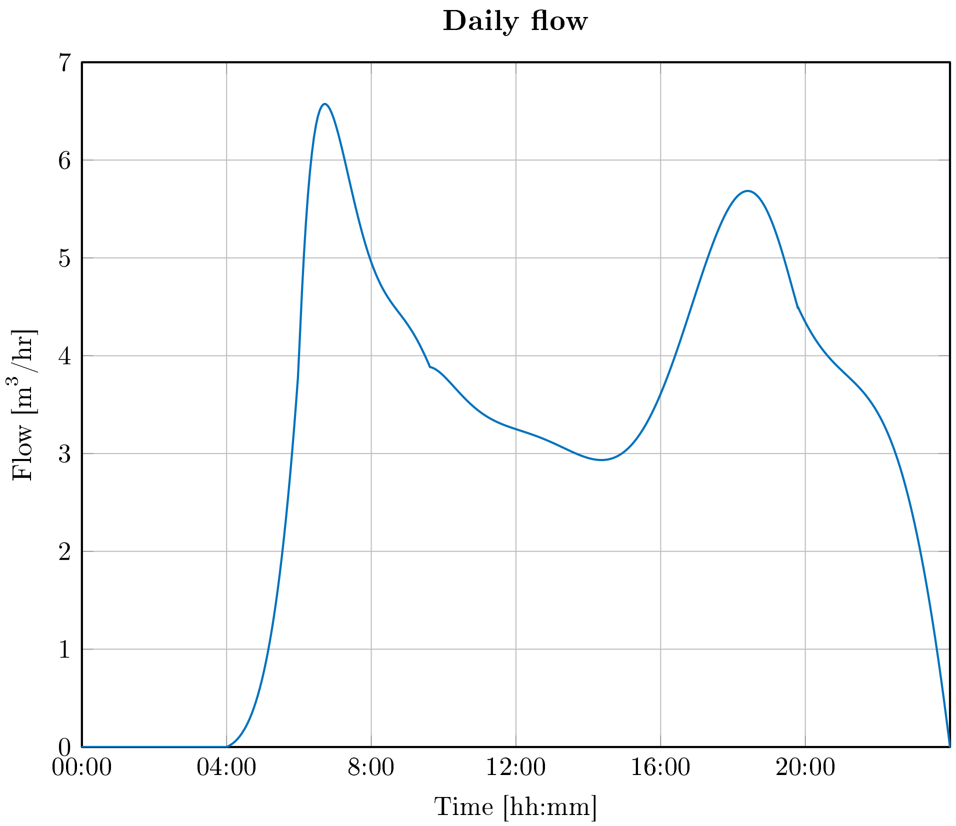

Figure A.4: A flow profile for Thulesvej.

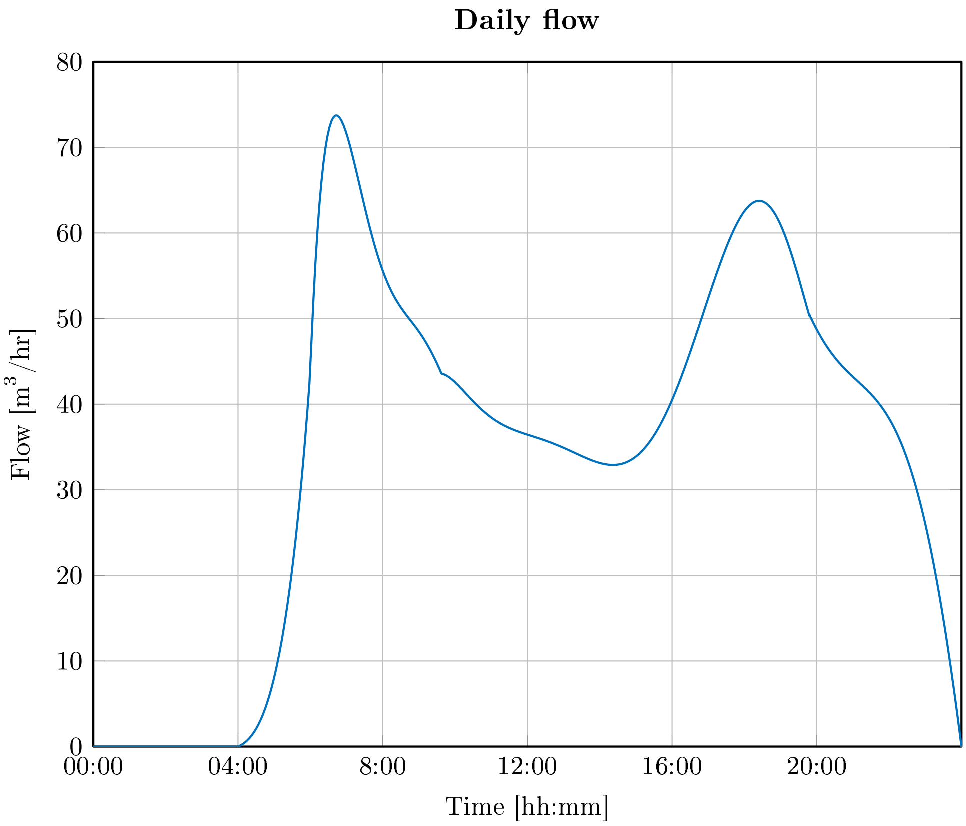

Figure A.5: A flow profile for Thulesvej.

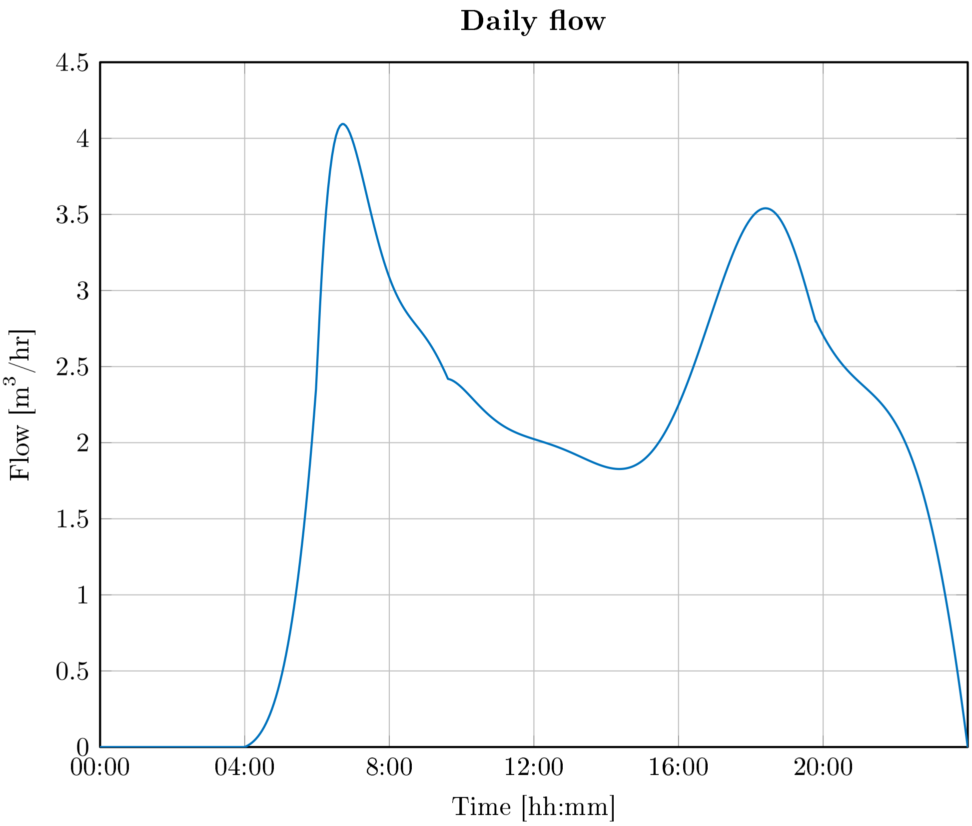

Figure A.6: A flow profile for Thulesvej.

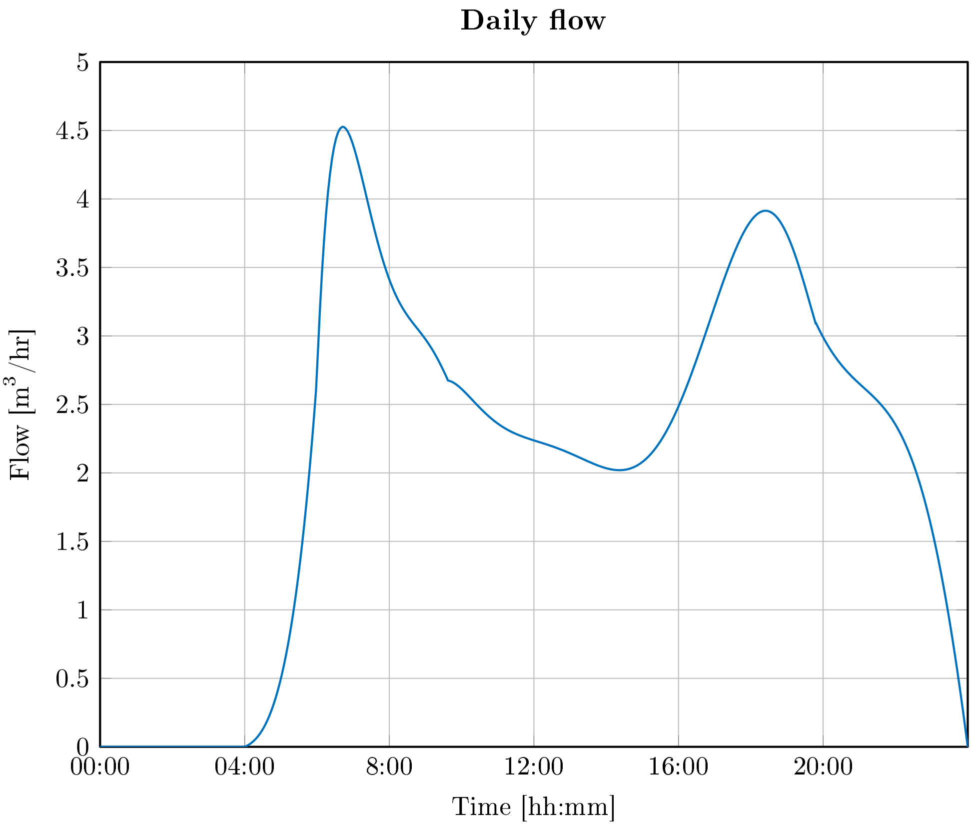

Figure A.7: A flow profile for Thulesvej.

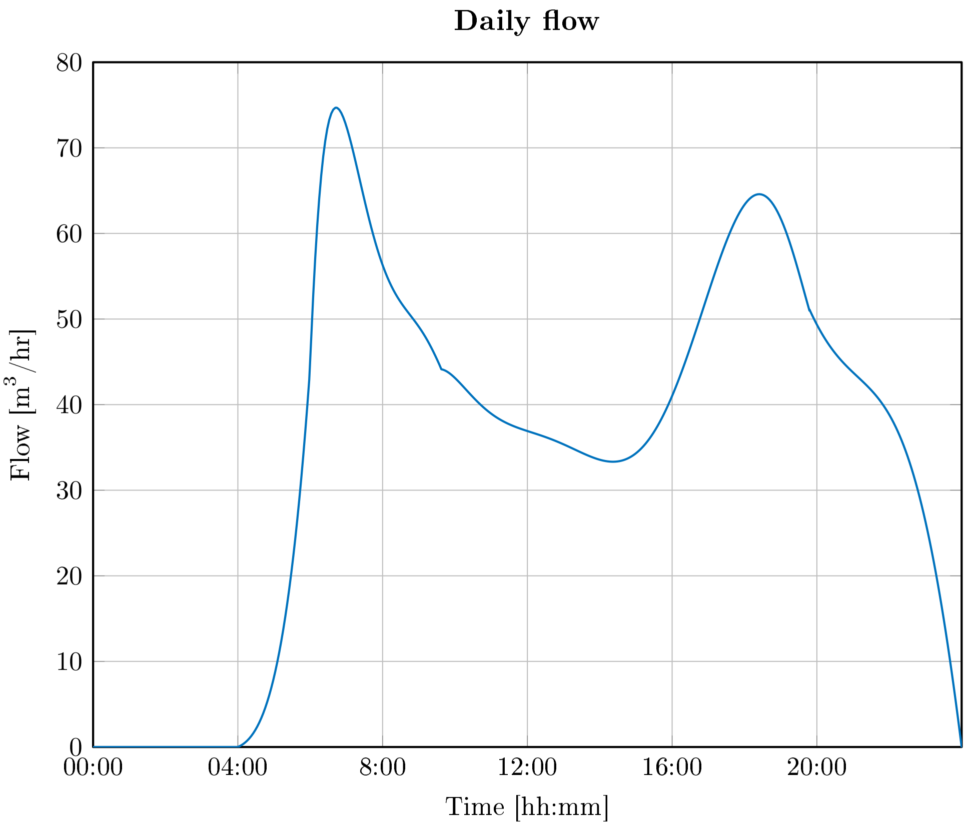

Figure A.8: A flow profile for Thulesvej.

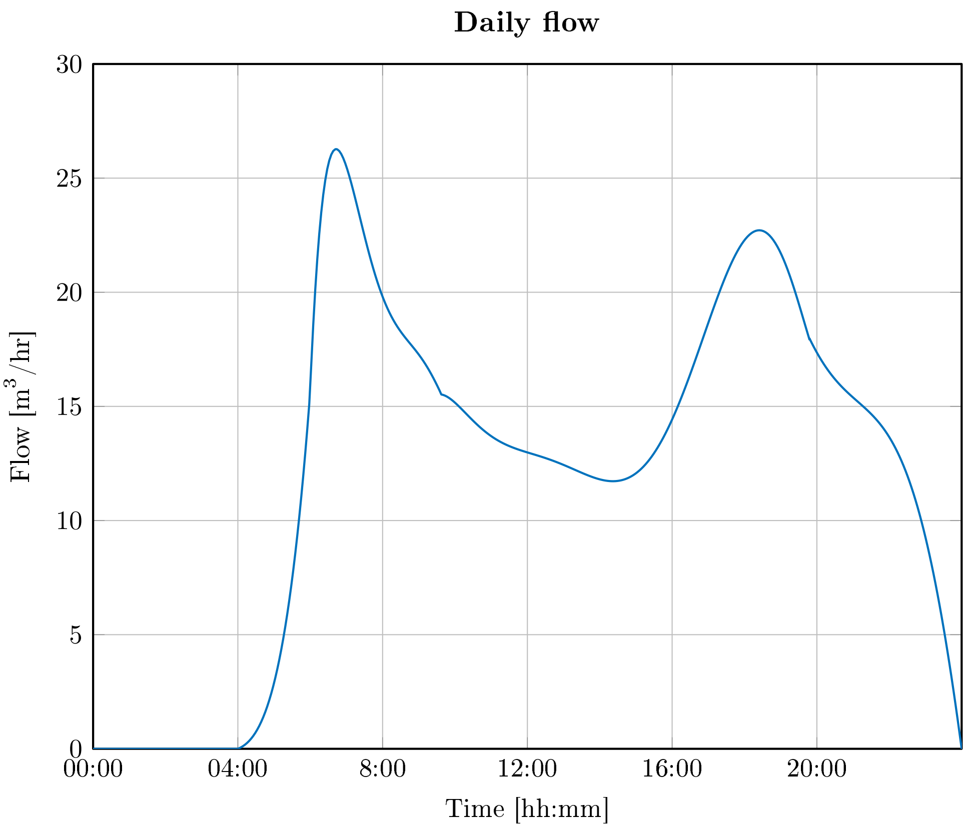

Figure A.9: A flow profile for Thulesvej.

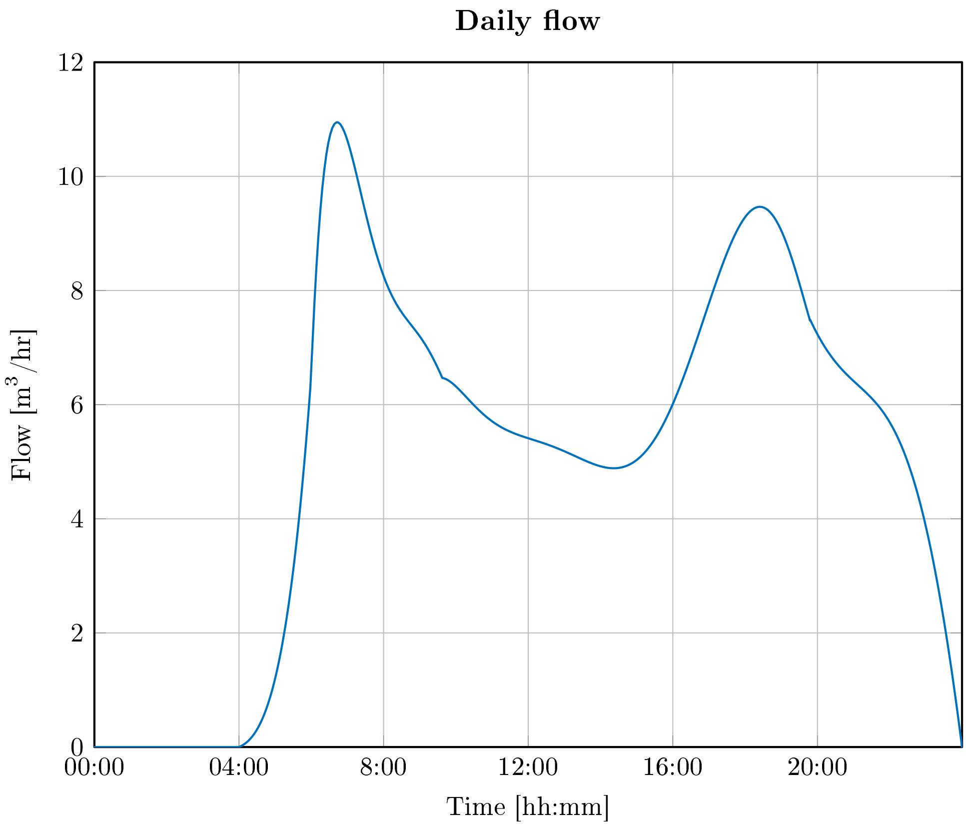

Figure A.10: A flow profile for Thulesvej.

A.4 Formulas

Rettelser